doi.org/10.36721/PJPS.2026.39.5.REG.14153.1

Development and optimization of mirtazapine loaded lipid-based transethosomal gel; *in-vitro*, *ex-vivo* and toxicological analysis

Faraz Ashraf[1], Hafiz Arfat Idrees[2]*, Minahal Munir[3] and Maaida Ajmal[1]
[1]Faculty of Pharmacy, The University of Lahore, Lahore, Pakistan.
[2]Faculty of Pharmacy and Biomedical Sciences, MAHSA University, Malaysia.
[3]Faculty of Pharmaceutical Sciences, The University of Central Punjab, Lahore, Pakistan.

Abstract: **Background**: Application of drugs through the transdermal route is preferable over other routes of drug delivery because of the ease of drug administration and reduced systemic side effects. Mirtazapine is a BCS class II noradrenergic and specific serotonergic drug and shows poor solubility and bioavailability. **Objective**: This study aims to develop and optimize a mirtazapine-loaded lipid-based transethosomal gel to enhance transdermal drug delivery and bypass first-pass metabolism. The current study is an attempt to minimize the systemic side effects associated with oral administration of mirtazapine and to avoid first pass metabolism by administering the drug through the skin. **Methods**: Transethosomes were formulated using the cold method and optimized via Box–Behnken design by varying phospholipid, surfactant, and ethanol concentrations. **Results**: The optimized formulation (F-16) exhibited high entrapment efficiency (75.92%) and cumulative drug permeation (73.62%) after 6 hours. Multiple characterization tests confirmed nano-sized, stable vesicles with a zeta potential of −34.1 mV and particle size of 479.3 nm. The transethosomal dispersion was incorporated into a Carbopol gel and evaluated for pH, viscosity, spreadability, drug content, and skin permeation. *Ex-vivo* studies showed enhanced skin permeation from the gel compared to the dispersion. Stability tests confirmed physical integrity over 60 days, while skin irritation and toxicological studies in animal models indicated excellent biocompatibility, with no signs of inflammation or organ toxicity. **Conclusion**: These findings and the study suggests that the transethosomal gel formulation is a promising and safe approach for transdermal delivery of mirtazapine, potentially improving its bioavailability and therapeutic effectiveness resulting in bypassing first pass metabolism.

Keywords: Box–Behnken design; Drug permeation; Entrapment efficiency; Mirtazapine; Transethosomes; Transdermal gel; Toxicological analysis

Submitted on 20-02-2025 – Revised on 16-06-2025 – Accepted on 07-08-2025

INTRODUCTION

The oral route remains the most frequently employed method for drug administration due to its convenience and ease of use (Kaminsky *et al.,* 2015). However, a significant limitation of oral delivery, particularly for drugs with poor aqueous solubility or high first-pass metabolism, is reduced bioavailability and erratic plasma concentration profiles (Ho, Jacob and Tangiisuran, 2017; Solmi *et al.*, 2020). These pharmacokinetic disadvantages may compromise therapeutic outcomes and patient adherence (Murata *et al.*, 2012). In contrast, the transdermal route bypasses hepatic metabolism, offers sustained drug release and improves pharmacokinetic predictability (Puri *et al.*, 2017). The stratum corneum layer is the major barrier that interferes with effective transdermal drug delivery. One technique to overcome this barrier includes the use of liposomes, mainly composed of phospholipid, for the transdermal delivery of drugs (Sudhakar *et al.*, 2021). However, the liposome's rigid structure prevented it from penetrating deeper into the skin, causing it to stay limited to the skin's outer layers (Franzé *et al.*, 2017). The problems associated with the rigid structure and hard membrane characteristic of liposomes were resolved with the development of deformable liposomes, called transferosomes (Opatha *et al*, 2020) by Cevc and Blume. After transferosomes, ethosomes were created (Touitou *et al.*, 2000) in which ethanol fluidizes the lipid membrane of the stratum corneum and interacts with the lipid layer of the vesicles thus making them more flexible.(Paiva-Santos *et al.*, 2021)

Transethosomes, a more recent advancement, are hybrid vesicular carriers that incorporate both ethanol and edge activators, thereby exhibiting the advantages of ethosomes and transferosomes concurrently. These vesicles exhibit enhanced elasticity, stability, and penetration depth across the stratum corneum, making them suitable for delivering lipophilic and hydrophilic agents (Song *et al.*, 2012; Akl, Eldeen and Kassem, 2024). Mirtazapine is a tetracyclic antidepressant primarily used in the treatment of moderate to severe major depressive disorder. It is classified as a Biopharmaceutics Classification System (BCS) Class II compound, possessing high permeability but low

**Corresponding author:* e-mail: hafizarfat@mahsa.edu.my

solubility. Its physicochemical characteristics include a partition coefficient (log P) of 2.9, a melting point of 114–116 °C, and a molecular weight of 265.4 g/mol. Despite favorable pharmacodynamics, mirtazapine demonstrates approximately 50% oral bioavailability, attributed to extensive hepatic first-pass metabolism and bitter organoleptic properties, which collectively present formulation challenges for oral administration (Kaur *et al.*, 2020).

In recent years, nano-vesicular drug delivery systems have been increasingly studied for central nervous system (CNS) medications, owing to their ability to enhance transdermal absorption and avoid hepatic first-pass metabolism (Teleanu *et al.*, 2019). Lipid-based carriers such as niosomes, transferosomes, and ethosomal gels (Yadav *et al.*, 2023) have been shown to improve dermal permeation and provide controlled drug release profiles for psychotropic compounds (Pires *et al.*, 2023) Despite this, no transethosomal formulation of mirtazapine has been reported in the current scientific literature. Given mirtazapine's unfavorable oral pharmacokinetics and its physicochemical suitability for dermal absorption, it represents a promising candidate for transdermal delivery. This study was therefore undertaken to develop and optimize a mirtazapine-loaded transethosomal gel using Box–Behnken Design. The optimized formulation was subsequently evaluated for its physicochemical characteristics, *in vitro* and ex vivo performance, and toxicological safety in accordance with standard analytical and histopathological protocols.

MATERIALS AND METHODS

Materials

Mirtazapine was obtained as a gift sample from a local pharmaceutical industry in Pakistan. Span 80, soya lecithin, ethanol, propylene glycol, Carbopol 940, methyl paraben, and propyl paraben were purchased from Sigma Aldrich, USA. All used chemicals and solvents were of analytical grade.

Formulation of mirtazapine transethosomes dispersion

Transethosomes were prepared by the cold method in which an organic and aqueous phase were separately prepared (Rai, Pandey and Rai, 2017). Organic phase was prepared by mixing soya lecithin and span 80 on a magnetic stirrer (VLEP, CHINA) at a speed of 1200 rpm. 30 mg of drug was dissolved in the required amount of ethanol. The resulting solution was vortexed on a vortex machine (MV-100) and sonicated on a sonicator (YR01256) and then added dropwise to the organic phase and stirred for 30 minutes on the magnetic stirrer. Aqueous phase was made by adding propylene glycol to the required quantity of water for volume makeup. The aqueous phase is then added dropwise to the organic phase. The resulting mixture was stirred for 30 minutes at 700 rpm. The final solution was then homogenized by a high shear homogenizer (HMG-500C) for 15 minutes with an interval of 5 minutes, followed by sonication. The prepared transethosomal dispersion was then stored for further characterization tests. The schematic representation of the methodology is shown in fig.1.

Box–Behnken Design was applied to optimize the formulation, using soya lecithin (X1), span 80 (X2), and ethanol (X3) as independent variables, while entrapment efficiency (Y1) and cumulative drug permeation at 6 hours (Y2) were set as response variables, as summarized in Table 1. In box-Behnken design, the minimum and maximum level refer to the coded levels of the independent variables.

Systematic optimization using Box - Behnken design

Different factors such as the amount of lipid (soya lecithin), concentration of surfactant (Span 80) and the percentage of ethanol were identified as the formulation parameters which could affect the properties of the transethosomes for the effective transdermal delivery (Qureshi *et al.*, 2023). Based on these findings, restrictions were established on each factor regarding how much they might influence the characteristics of the formulation. The Response Surface Methodology was employed by using Design Expert ver. 12 software.

The design consisted of the 15 experimental trials (Table 2) with the computer-generated quadratic model as follows:

$$Y = b_0 + b_1 X_1 + b_2 X_2 + b_3 X_3 + b_{12} X_1 X_2 + b_{13} X_1 X_3 + b_{23} X_2 X_3 + b_{11} X_1^2 + b_{22} X_2^2 + b_{33} X_3^2$$

Y is the measured response related to each factor level; b_0 is a constant; b_1, b_2, b_3 are the linear coefficients; b_{12}, b_{13}, b_{23} are coefficients of interactions among three factors; b_{11}, b_{22}, b_{33} are the quadratic coefficients of observed experimental values and X_1, X_2 and X_3 are the mentioned levels of independent variables. Selected independent variables were soya lecithin (X_1), Span 80 (X_2) and ethanol (X_3) and the dependent variables were entrapment efficiency (Y_1) and cumulative amount of drug permeation (Y_2). The experimental trials designed by Box Behnken Design were formulated by the previously described method and all the prepared formulations were evaluated for the entrapment efficiency and amount of drug release at Q6h.

Drug entrapment efficiency (%EE)

Cold centrifugation method was used in which 0.2 ml transethosomal dispersion was placed in the centrifuge machine (CE-5A) and the column was cool centrifuged at 20,000 rpm for 30 minutes at 4 ± 0.5°C. Supernatant was collected, dissolved in methanol and sonicated for 12 minutes which was then examined by using a UV-VIS Spectrophotometer (Halo DB-20) at λ_{max} of 222nm. Equation 1 was used to estimate the percentage drug

entrapment efficiency (%EE) (Acharya, Ahmed and Rao, 2016):

% EE = amount of entrapped drug / total amount of drug × 100 (equation 1)

Amount of drug permeation after 6 hours/360min (Q 6h)

A phosphate buffer solution of 7.4 pH was used and maintained at 37 ± 0.2°C in a Franz diffusion cell (FDC) (LEDC-03) having a surface area of 3.14 cm^2 and a capacity of 10ml. Rabbit was sacrificed and its skin had been preserved overnight in PBS (pH 7.4) at 4 ºC . The skin was attached at the base of the donor compartment and 1 ml of the prepared transethosomes formulation was put over the skin (Moolakkadath *et al.*, 2018). The sample (1 ml) was removed at predefined intervals of 60, 120, 180, 240, 300 and 360 minutes (1, 2, 3, 4, 5 and 6 hours) and sink conditions were maintained. Samples were then filtered by using a 0.20-µm membrane filter and examined at a λ_{max} of 222nm on a UV-VIS spectrophotometer (Fang *et al.*, 2006).

Selection of the optimized formulation of transethosomes dispersion

The criteria for selecting the optimized formulation were based on the highest entrapment efficiency (EE%, Y1) and cumulative drug release at 6 hours (Q6h, Y2). Statistical analysis of the 15 experimental formulations was conducted using Design Expert® software, employing a two-factor, three-level Box-Behnken design. Analysis of variance (ANOVA) confirmed the significance of the model ($p < 0.05$), and the polynomial equations generated for each response predicted how formulation variables influenced Y1 and Y2. Although F-8 showed the highest EE% (86.5%) and F-13 had the highest Q6h (86.7%), no single formulation simultaneously maximized both responses. Therefore, a desirability function approach was applied, which mathematically combines multiple response criteria. Based on this composite desirability score (0.981), formulation F-16 was selected as the optimized batch, as it achieved a balanced compromise between high EE% and optimal drug release.

The desirability function approach was used based on the results of the studied variables to select the optimized formulation (Moolakkadath *et al.*, 2018). After numerical optimization by using Design Expert software, the best selected solution with the highest desirability (0.981)) was chosen as the optimized formulation of transethosomes dispersion (F-16). Table 3 presents the composition of the optimized transethosomal formulation (F-16), along with the (EE%) and (Q6h) for both the predicted and experimentally prepared formulations.

The optimized formulation (F-16) exhibited an EE% of 75.92% and a Q6h value of 73.62%, which are in close agreement with the predicted values of 77.13% and 74.62%, respectively, as obtained from the Design Expert® software.

Characterization of the optimized transethosomes dispersion (F-16)

Following characterization tests are performed on the optimized transethosomes dispersion:

UV-spectrophotometric method for quantification of mirtazapine

Preparation of stock solution

100 mg of mirtazapine is dissolved in 10 ml of ethanol followed by the sonication for 10 minutes. Distilled water is used for the volume makeup to obtain the 100 µg/ml concentration and the final solution is then filtered.

Preparation of standard solutions

To get a 10-50 µg/ml concentration, aliquots from the stock solution were taken and diluted with water and analyzed on UV-VIS spectrophotometer at the wavelength of 222nm. Calibration curve was obtained by plotting the concentration of the standard solution on the horizontal x-axis and absorbance on the y-axis (Bendale *et al.*, 2011).

Zeta potential, polydispersity index (PDI) and particle size determination

Transethosomes vary in size from tens of nanometers to microns, which is dependent upon the formulation excipients. Zeta potential is a valuable and important measure of particle surface charge that can be used to anticipate and control stability. The size of the particles was determined by using a Malvern Zetasizer (Malvern Instruments Ltd., Worcestershire, UK). Polydispersity is the ratio of a droplet's standard deviation to its mean size. The higher the polydispersity value, the less homogeneous the droplet size in the formulation. The size, zeta potential and PDI of the particles were determined by using a Zetasizer. Optimized formulation was diluted with distilled water and placed in a cuvette (Gunasekara *et al.*, 2015).

Scanning electron microscopy (SEM)

SEM is used as a primary technique to investigate the three-dimensional structure of the formulation. The prepared sample was put on the grid with a working distance (WD) of 8.5 mm and a width of 19.05 µm. The material was then tested at various magnifications.

Drug excipients compatibility study

Fourier Transform Infrared Spectroscopy (FTIR) is commonly used to assess the compatibility of active pharmaceutical ingredients (APIs) with excipients by identifying functional groups and monitoring potential physical or chemical interactions. Changes in peak intensity, the appearance of new peaks, or shifting of characteristic absorption bands may suggest possible interactions between the drug and excipients (Bharate,

Bharate and Bajaj, 2010). In this study, FTIR spectra were recorded using an FTIR-7600 (Lambda Scientific, Australia) over a wavenumber range of 600 to 4000 cm^{-1}. The analysis was conducted using PC-based software for spectral processing and interpretation. While FTIR is a valuable tool for evaluating functional group behavior, it does not confirm drug entrapment within vesicles.

X-ray diffraction (XRD)

This method is used for determining the crystalline nature and phase composition. X-ray diffraction of pure drug and the optimized transethosomal formulation was conducted by using Xray diffractometer. After being scanned at a speed of 3°/min, the samples were tested between 5° and 80° (2θ).

Differential scanning calorimetry (DSC) and thermogravimetric analysis (TGA)

DSC and TGA were performed to determine the thermal stability of the formulation (Demetzos, 2008). The pure drug and optimized transethosomal formulation were thermally analyzed using a DSC and TGA analyzer. Sample was placed in an aluminum pan and from the DSC and TGA thermograms of samples, transition temperature was observed.

Drug content

1 ml of the prepared formulation was diluted with the 10 ml of phosphate buffer having pH 7.4 to determine the drug content. This solution was stirred for 2 hours and the sample was filtered by using filter paper. It was then examined at 222 nm on a UV-VIS spectrophotometer.

Release kinetics

Drug release kinetics was calculated by models, including the Korsmeyer-Peppas (Wu *et al.*, 2019), Hixson-Crowell (Hamedi *et al.*, 2019), zero-order (Miastkowska *et al.*, 2016), first-order (Kadakia, Shah and Amiji, 2017) and Higuchi model (Cong *et al.*, 2017). DD solver software was used to assess the release kinetics and the R^2 values were determined for each model to find out the drug release pattern of the formulations.

Preparation of the transethosomes vesicular gel

Optimized transethosomes dispersion (F-16) was incorporated into the Carbopol gel for easy application onto the skin. Carbopol 934 (1% w/v) was soaked in a suitable amount of distilled water overnight. 30 ml of transethosomal dispersion containing 30 mg of mirtazapine drug was added to the swollen polymer while being continuously stirred until a homogeneous gel was formed. Propyl paraben and methyl paraben were added as preservatives and the triethanolamine was added dropwise to the gel to bring the pH to neutral (Garg *et al.*, 2017). The final concentration of mirtazapine in the gel formulation was fixed at 0.45% (Pintea *et al.*, 2022). Final composition of the prepared gel is given in the table 4.

Characterization of the mirtazapine loaded transethosomal gel

Organoleptic Evaluation

The clarity and appearance of the gel were evaluated visually in a separate container to determine the presence of lumps and aggregates. Any signs of grittiness and agglomeration in the prepared gels were observed (Abdallah *et al.*, 2022).

pH

It was measured by using the digital pH meter and all values were taken at room temperature (25 °C). The formulation's pH should range from 5.0 - 6.5 to match the pH of skin (Shah *et al.*, 2019).

Viscosity measurement

Viscosity affects the drug release from the formulation. Additionally, the viscosity affects the semisolid dosage forms' stability, spreadability, release of drugs, and ease of application. A beaker was filled with a specific amount of the prepared formulation, and it was left to settle for thirty minutes at room temperature. The spindle dropped into the formulation and rotated at a speed of 20 revolutions per minute. Average of three readings of the viscosity was noted and viscosity is measured in centipoise units (Tiwari *et al.*, 2021).

Spreadability

Spreadability is important to determine the even distribution of the prepared formulation (Asad *et al.*, 2021). 2 gm of gel was applied to one side of a glass slide and another slide was placed above it. Weight of 100 grams was placed on the upper slide for 5 minutes. The time taken to separate the upper glass slide away from the lower glass slide was noted. Spreadability can be measured by the formula given in equation 2.

S = M/t (equation 2)

Where "t" is the time taken by the gel in seconds, "M" is the weight of the gel in grams, and "S" stands for spreadability in grams per second (g/s).

Drug content assessment

0.5 g of transethosomal gel was diluted to ten milliliters with accurately weighed quantity of ethanol. After passing the mixture through Whatman filter paper, mixture was agitated for a period of one hour. At a wavelength of 222 nm, the drug's content was analyzed spectrophotometrically in comparison to a blank sample that included the same excipients but no medication (Abdelnabi et al., 2019). The drug content was measured by applying the calibration curve developed by same solvent previously used for dilution of transethosomal gel.

Formula in equation 3 was used to calculate the percentage drug content. The drug was detected by using the calibration curve.

% Drug content = absorbance of test / absorbance of standard × 100 (equation 3)

Table 1: Independent variables with their levels and dependent variables with constraints in Box Behnken design

Variables	Level	
	Minimum	Maximum
Independent variables		
X1 = Soya lecithin (mg)	2	4
X2 = Span 80 (mg)	10	30
X3 = Ethanol (%)	20	50
Drug	30 mg (fixed in all formulations	
Dependent variables		
Y1 = Entrapment efficiency (%)	Maximize	
Y2= Cumulative amount of drug permeation after 6 hours (Q 6h)	Maximize	

Table 2: Experimental formulation design and measured responses based on Box–Behnken methodology (n=3,±SD)

Formulations	Independent variables			Dependent variables	
	X_1(mg)	X_2 (mg)	X_3(%v/v)	Y_1(%)	Y_2(%)
F-1	3	30	50	65.20±1.11	69.3±1.75
F-2	4	30	35	73.9±1.02	65.4±1.33
F-3	2	10	35	75.6±1.67	57.6±1.64
F-4	3	10	50	69.3±1.56	70.2±1.96
F-5	2	20	50	61.6±1.85	76.8±1.25
F-6	3	20	35	72.5±1.96	74.4±1.64
F-7	3	20	35	72.5±1.26	74.4±2.06
F-8	3	10	20	86.5±1.24	49.9±1.69
F-9	3	20	35	72.5±2.01	74.4±1.32
F-10	2	30	35	63.3±1.59	56.2±1.48
F-11	4	20	20	80.5±1.57	63.9±1.74
F-12	4	10	35	77.9±2.11	67.2±1.65
F-13	4	20	50	67.8±1.69	86.7±2.04
F-14	2	20	20	70.8±1.27	58.9±1.63
F-15	3	30	20	71.6±1.64	47.1±1.28

X_1: Soya lecithin (mg), X_2: Span 80 (mg), X_3: ethanol (%), Y_1: entrapment efficiency (%), Y_2: total amount of drug permeated at 6 hours (%).

Table 3: Composition of the optimized formulation (F-16) and validation of the responses

Optimized formulation	Independent variables			Dependent variables	
	X_1 (mg)	X_2 (mg)	X_3 (%v/v)	Y_1 (%)	Y_2 (%)
F-16 Predicted formula	4	16.8	31.83	77.130	74.924
F 16 Practically prepared formula	4	16.8	31.83	75.924	73.62

Table 4: Composition of mirtazapine-loaded transethosomal gel formulation

Ingredients	Concentration
Carbopol 934	1% w/v
Propyl paraben	0.01 % w/w
Methyl paraben	0.01 % w/w
Triethanolamine	Added dropwise to adjust pH
Distilled water	q. s

Table 5: Assessment scale for erythema

Score	Grade of erythema	Explanation
0	Clear	No sign
1	Almost clear	Little redness
2	Mild	Definite redness indicating mild erythema
3	Moderate	Moderate erythema marked redness
4	Severe	Intense redness indicating severe erythema

Drug release

2 ml of transethosomal dispersion was incorporated into the high-flux dialysis membrane (14 kDa)and drug release was measured by using USP dissolution apparatus II containing 500 ml of phosphate buffer solution of 7.4 pH maintained at 37°C (Albash *et al.*, 2019). The paddle was adjusted to rotate at 50 rpm. Aliquots of 10ml were taken out at a predefined interval for a total period of 6 hours and replaced with fresh buffer. The samples were filtered through a syringe filter of 0.45µm and assessed spectrophotometrically at 222 nm wavelength (Yıldız *et al.*, 2016).

Ex-vivo skin permeation study

An ex-vivo skin permeation study was carried out to compare the transdermal drug delivery efficiency of the optimized transethosomal dispersion (F-16) and its gel formulation. Full-thick abdominal skin was excised from a sacrificed rabbit, after obtaining the letter of confirmation from the University's ethical committee vide letter no. IREC-2023-48. The rabbit skin was carefully cleaned, and stored in phosphate-buffered saline (PBS, pH 7.4) at 4 °C for use within 24 hours.

The skin was mounted between the donor and receptor compartments of a FDC, with the stratum corneum oriented toward the donor side. The receptor compartment (10 mL) was filled with PBS (pH 7.4) and maintained at 37 ± 0.5 °C under continuous magnetic stirring. One milliliter of each test formulation was applied to the donor compartment. Samples (1 mL) were withdrawn from the receptor compartment at predetermined intervals (1, 2, 3, 4, 5, and 6 hours) and immediately replaced with an equal volume of fresh PBS to maintain sink conditions.

The amount of mirtazapine permeated was quantified spectrophotometrically at λ_{max} = 222 nm (Musallam *et al.*, 2022) The percentage drug release and cumulative permeation profiles were calculated and compared between both formulations.

Stability studies

The stability of the prepared transethosomal gel was assessed by measuring its color, pH, viscosity, spreadability, and drug content. The gel under investigation was kept for 60 days at two different temperatures, 25 ± 0.5 °C and 4 ± 0.5 °C. The variables were routinely checked at intervals of 0, 15, 30, 45, and 60 days (Shah *et al.*, 2019).

Skin irritation study

The adult male rats were used in the skin irritation study. A point on the back of rat was marked and the hairs were removed using razor to examine the irritability of the gel formulation. After applying gel once daily for three days, skin sensitivity reactions such as redness, edema, and skin rash were observed to measure the level of skin irritation caused by the formulation. Grading level of the skin irritation is given in table 5 (Gao *et al.*, 2019).

Toxicology and histopathology

Albino rabbits weighing 800 g to 1200 g male and female had been brought from animal house at the University of Lahore, Pakistan after obtaining the letter of confirmation from the University's ethical committee vide letter no. IREC-2023-48. Two groups (control group and treatment group) with equal quantity of female as well as male rabbits (n=4) had been kept in a clean environment (clean housing facility), provided with 12-hour light and dark cycle. They were fed with a water and a regular meal. Only the treatment group received the mirtazapine loaded transethosomal gel on the back for two weeks twice a day. After fourteen days, hematological and clinical biochemistry analyses were performed.

RESULTS

Optimization of transethosomes by Box-Behnken design

A total of 15 experimental trials were generated by the Box-Behnken Design for the formulation development. Table 2 represents the values of entrapment efficiency and the drug permeation after six hours for all 15 formulations. Fig. 2 represents the entrapment efficiency and fig. 3 represents the total amount of drug permeation after 6 hours (Q 6h) of all the prepared experimental formulations. The values of R^2, S.D and % CV of each response are represented in Table 6.

Response surface analysis for the selection of optimized transethosomes formulation

The impact on the dependent variables was investigated using 3D surface plots, contour plots, and polynomial equations. ANOVA was applied to establish the statistical significance. The accuracy of the model is confirmed by the ANOVA as shown in Table 7.

Response 1 (Y_1): effect of independent variables on the entrapment efficiency

Impact of independent variables on the EE% is shown in fig. 4. Below is a polynomial equation displaying the final mathematical model in terms of coded factors as decided by the Design-Expert software (equation 4):

$$EE\ \%\ (Y1) = 87.50 + 3.35\ A - 3.85\ B - 4.85\ C + 1.43\ AB - 1.23\ AC + 1.82\ BC - 0.69\ A^2 + 1.06\ B^2 - 1.54\ C^2 \quad \textit{(equation 4)}$$

Where A represents the lipid, B represents the surfactant, C represents the ethanol; AB, BC, and AC is the interactions between factors; A2, B2 and C2 are the curvatures. Equation 4 and fig. 4 showed that the phospholipid (factor A) had a positive impact on the EE% of the drug, whereas the concentration of surfactant (factor B) and ethanol (factor C) had a negative impact on the entrapment efficiency.

Response 2 (Y_2): effect of independent variables on the amount of drug permeated after six hours

The impact of independent variables on Q6h is shown in fig. 5. Final mathematical model is shown in polynomial Equation (equation 5):

$$Q6h\ (Y2) = 74.40 + 4.21\ A - 0.86\ B + 10.40\ C - 0.10\ AB + 1.23\ AC + 0.48\ BC - 0.18\ A^2 - 12.63\ B^2 - 2.65\ C^2 \quad \text{(equation 5)}$$

Equation (5) revealed that the concentration of lipid (factor A) and the ethanol (factor C) had a positive impact on the amount of drug permeated after 6 hours (Q6h).

Characterization of optimized transethosomes formulation (F-16)

Calibration curve

The standard calibration curve for mirtazapine is shown in fig. 6

Zeta potential, PDI and particle size determination

Particle size, PDI and zeta potential of the optimized formulation were determined by the zeta sizer. Zeta potential of the optimized formulation is demonstrated in fig. 7.

Scanning electron microscopy (SEM)

The structure of the prepared transethosomal dispersion was studied by the scanning electron microscope at two different resolutions as shown in figs. 8 (a) and 8 (b).

Drug excipients compatibility study

The data of infrared transmittance for all the samples was screened over a wave number between 600 to 4000 cm^{-1}. The FTIR spectrum of the excipients and the final formulation are shown in the fig. 9.

X-ray diffraction (XRD) analysis

This test is most commonly used for determining the crystalline structure of a prepared product fig. 10 shows the XRD graphs of the pure drug and the prepared transethosomal formulation.

Thermal stability analysis (DSC/TGA)

Differential scanning calorimetry (DSC), along with thermogravimetric analysis (TGA), was used to evaluate the physical state and thermal stability of mirtazapine in the transethosomal formulation. TGA/DSC graphs of pure mirtazapine drug and the final transethosomal formulation are mentioned in the figs. 11(a) and 11(b) respectively.

Release kinetics

R^2 value of mirtazapine loaded transethosomes for different kinetics models is given in table 8.

Characterization of the mirtazapine loaded transethosomal gel

Organoleptic evaluation

The transethosomal gel was physically and visually inspected for different variables such as color, consistency, homogeneity, clarity, phase separation and grittiness. These results are given in Table 9.

pH, viscosity and spreadability

The values for pH, viscosity and spreadability of the prepared transethosomal gel were measured.

Drug content assessment

Mirtazapine -loaded transethosomal gel has a drug content percentage of 91.28% and drug content lies within the permissible limit of 100 ± 10%.

Drug release

The % drug release pattern from the optimized transethosomal dispersion (F-16) and the plain gel was determined up to 6 hours (360 minutes) as shown in fig. 12.

Ex-vivo permeation study

A permeation study of the transethosomal gel was conducted on the FDC using rabbit skin. fig. 13 shows the drug permeation through transethosomal gel for the period of six hours (360 minutes)

Stability studies

The results of the stability study of the mirtazapine loaded transethosomal gel is given in table 10.

Skin irritation study

The purpose of the skin irritation investigation was to verify that the gel formulation was safe and compatible with the rats' skin. Application of the mirtazapine loaded transethosomal gel on the rat's skin is represented in fig. 14.

Toxicology and histopathology

Histopathological analysis is shown in the fig. 15.

DISCUSSION

Optimization of transethosomes by Box-Behnken design

The values for two dependent variables, namely entrapment efficiency and drug permeation after 6 hours were in the range of 61.6 % to 86.5 % and 47.1 % to 86. 7 % respectively as shown in Table 2. Quadratic model was found to be most appropriate fit model for the responses of all 15 formulations

Response surface analysis for the selection of optimized transethosomes formulation

The model generated for the entrapment efficiency (Y_1) had a p-value of less than 0.05 and an F-value of 136.42 implies that the model is significant as shown in table 7. Similarly, the model generated for the drug permeation after 6 hours had a p-value of less than 0.05 and an F-value of 385.56 which indicated the significance of model.

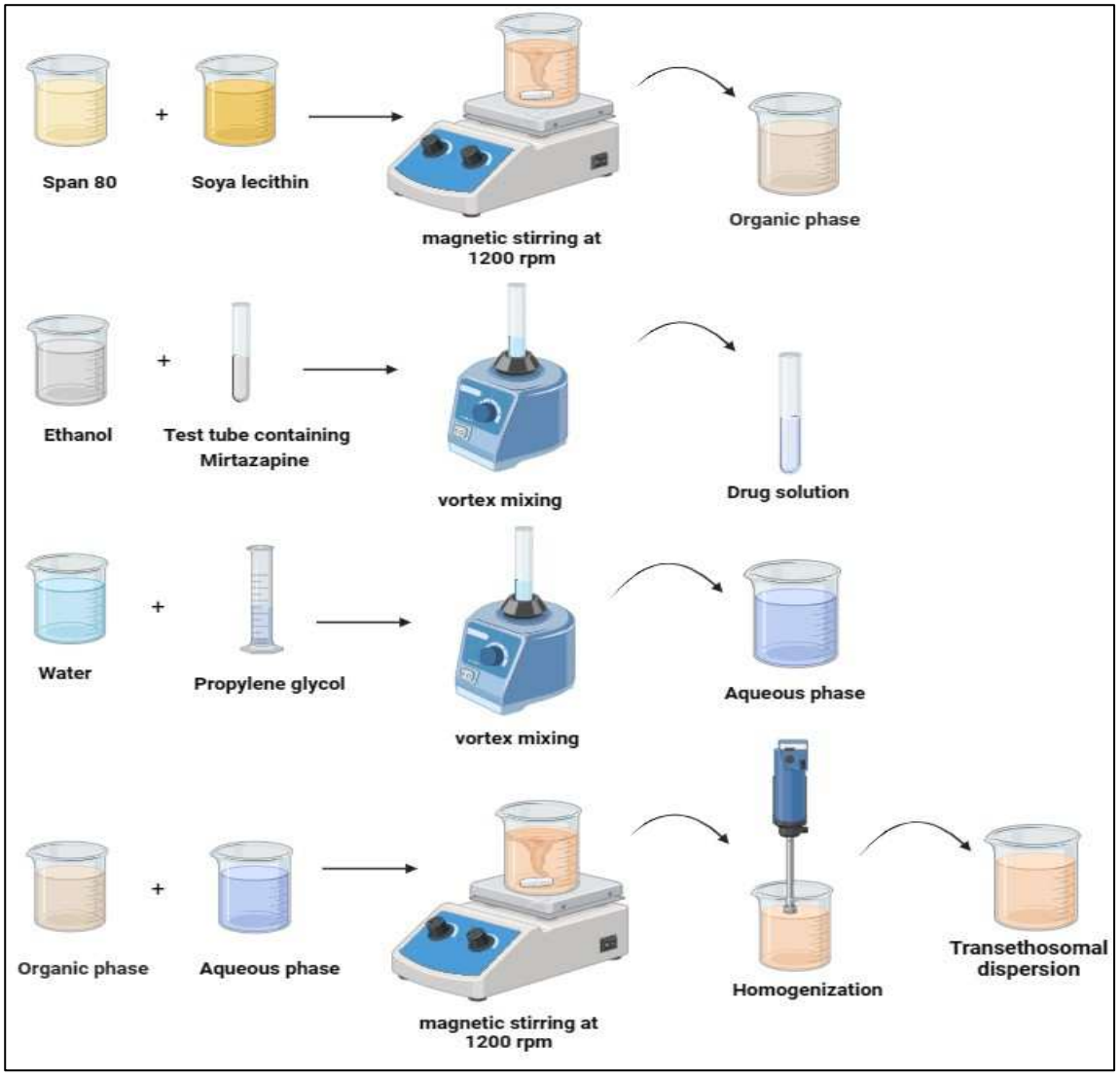

Fig. 1: Stepwise representation of the preparation of mirtazapine-loaded transethosomes and their incorporation into carbopol-based gel

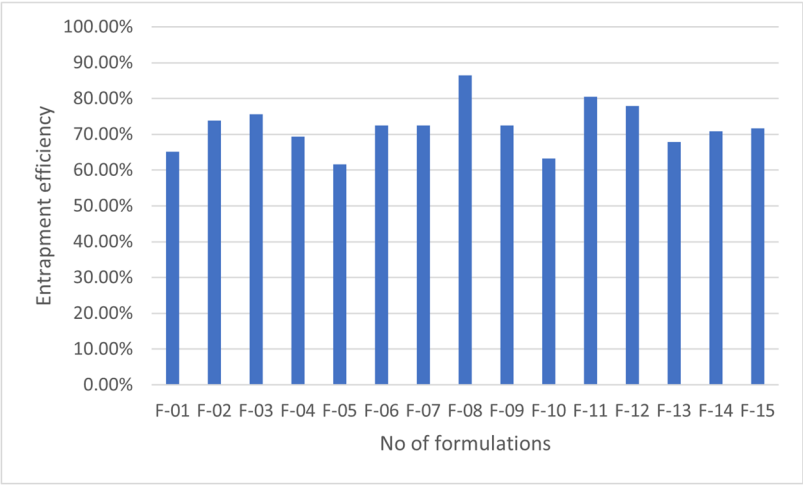

Fig. 2: Comparative entrapment efficiency of Box–Behnken-designed transethosomal formulations (F-1 to F-15)

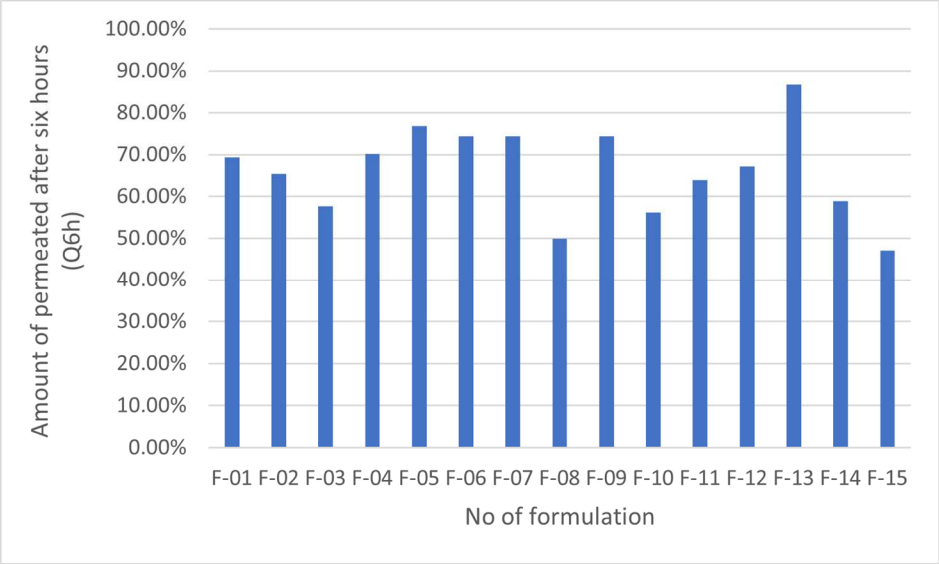

Fig. 3: Cumulative drug permeation at 6 hours (Q6h) for formulations F-1 to F-15

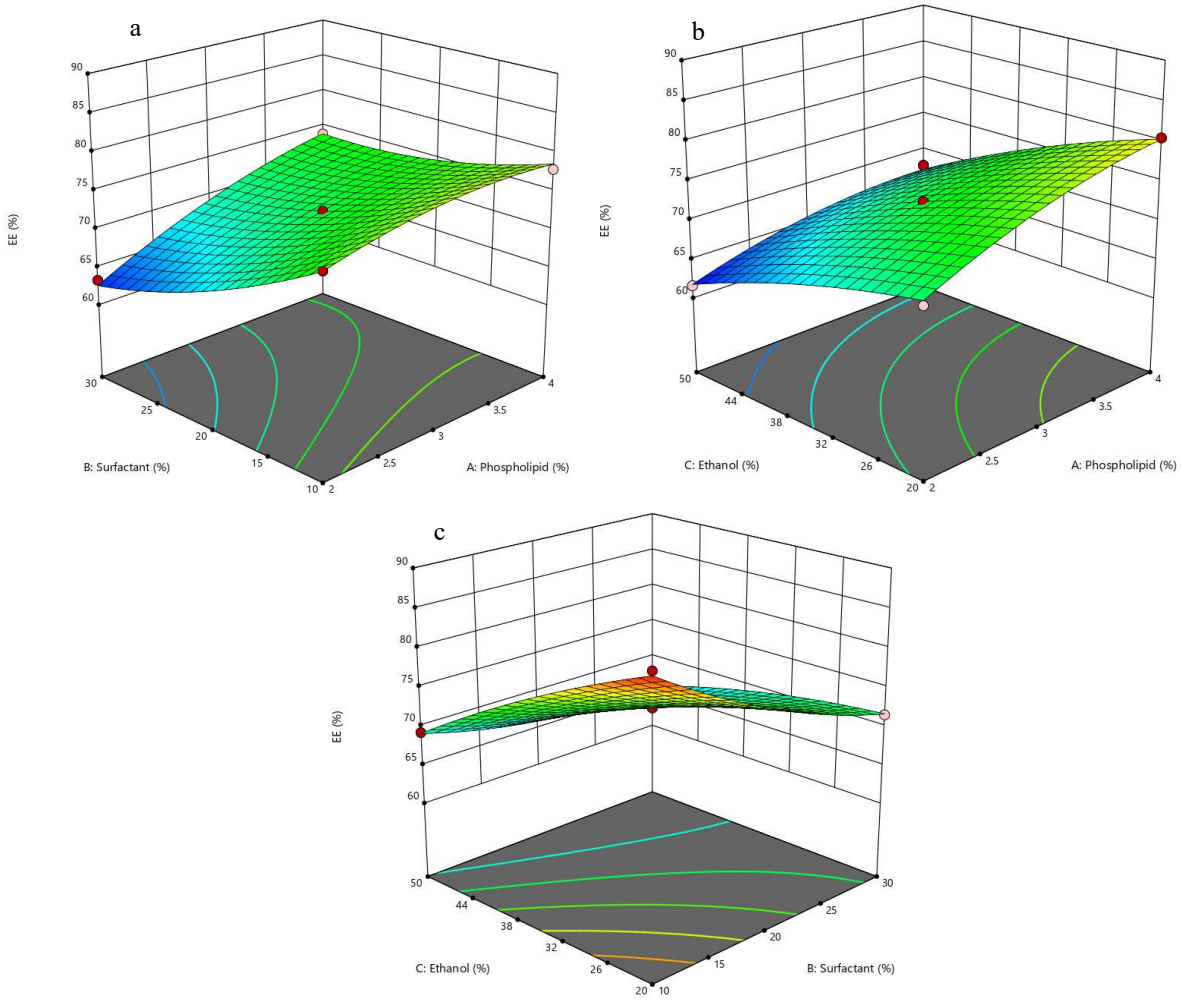

Fig. 4: Three-dimensional response surface graph represents the impact of independent variables on entrapment efficiency EE% (Y1); (a) represents the impact of Surfactant and Phospholipid on EE%, (b) represents the impact of Phospholipid and Ethanol on EE%, (c) represents the impact of Ethanol and Surfactant on EE%

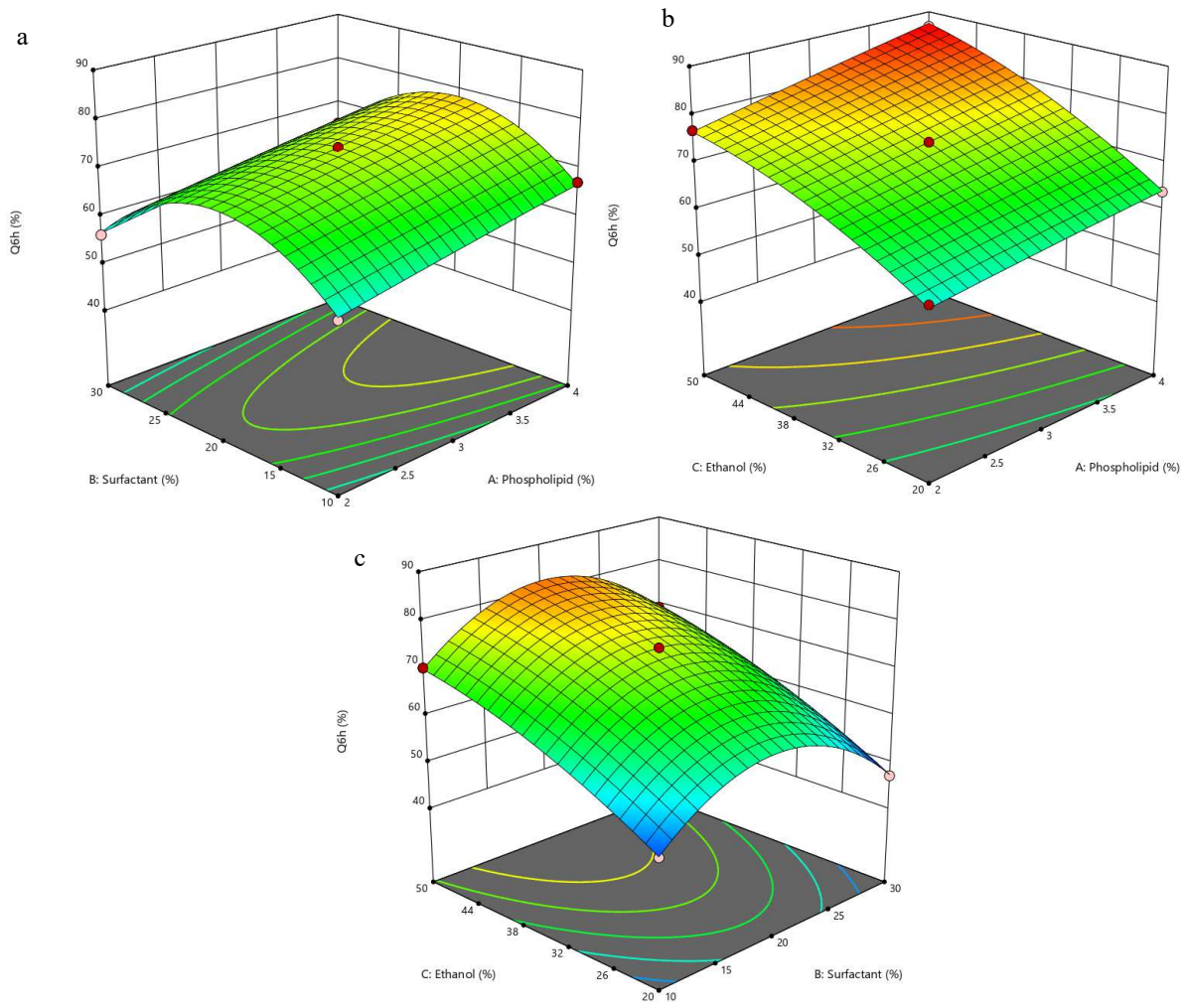

Fig. 5: Three-dimensional response surface graph showing the effect of independent variables on the cumulative amount of drug after 6 hours (Y2); (a) represents the impact of Surfactant and Phospholipid on Q6h, (b) represents the impact of Phospholipid and Ethanol on Q6h, (c) represents the impact of Ethanol and Surfactant on Q6h

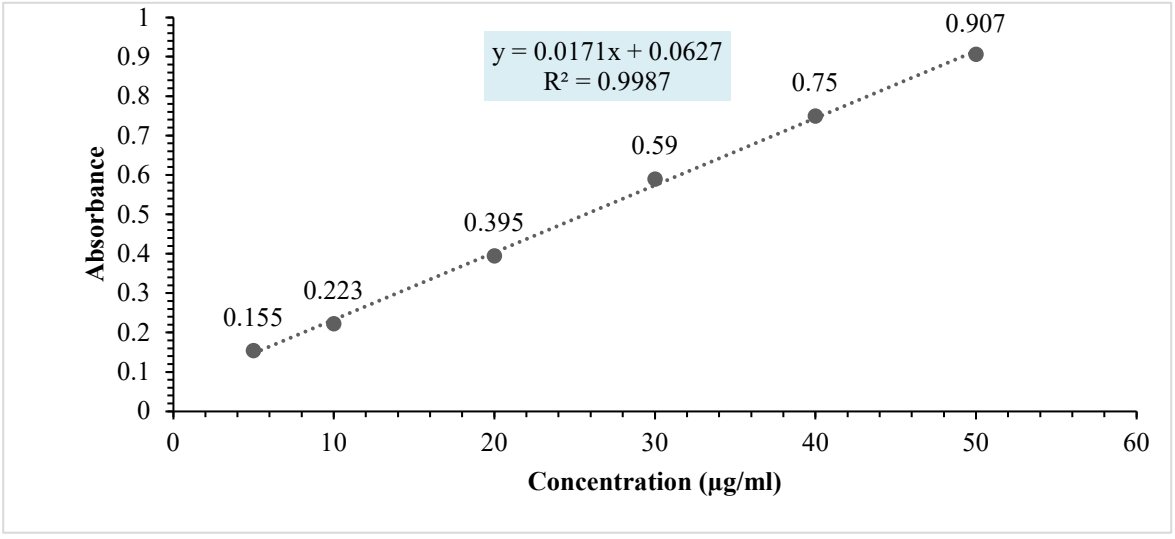

Fig. 6: Calibration curve of Mirtazapine

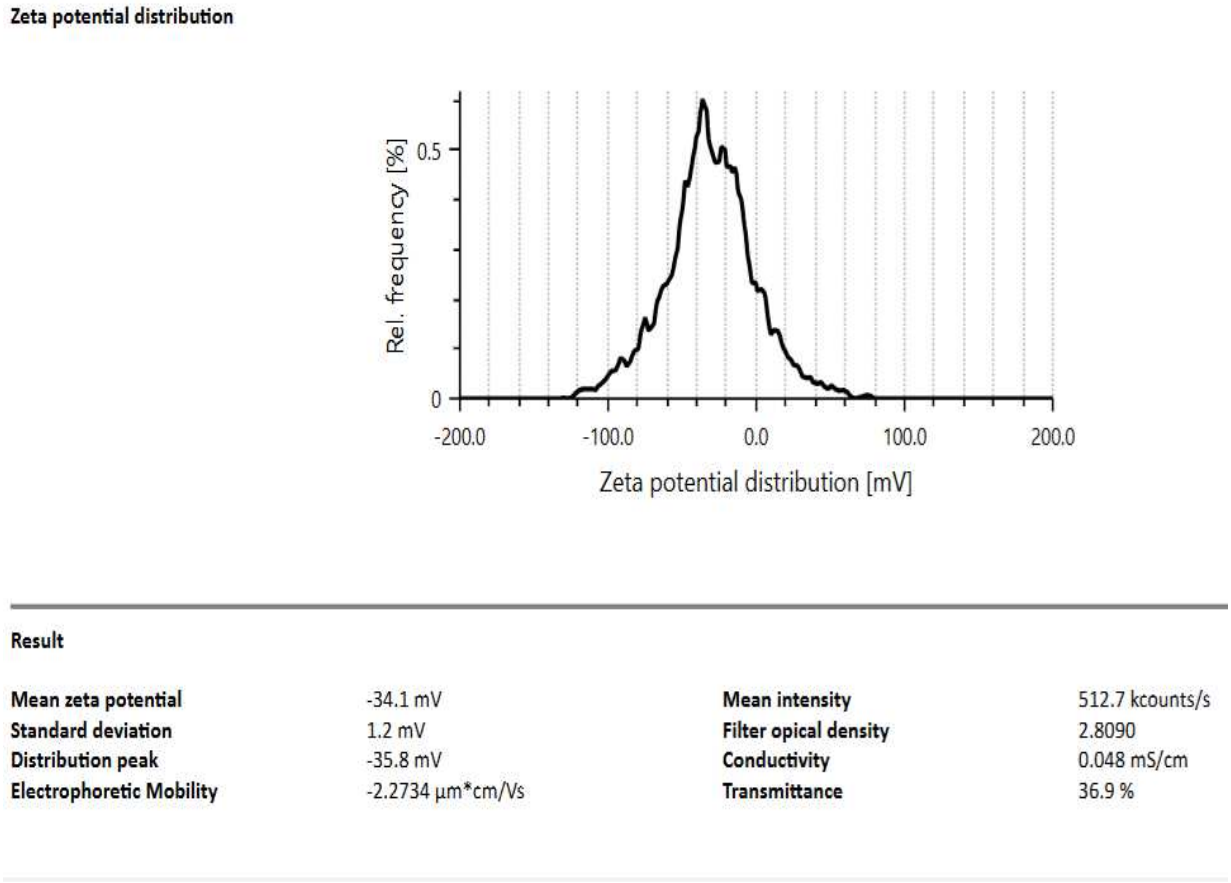

Fig. 7: Zeta potential of the optimized transethosomal dispersion

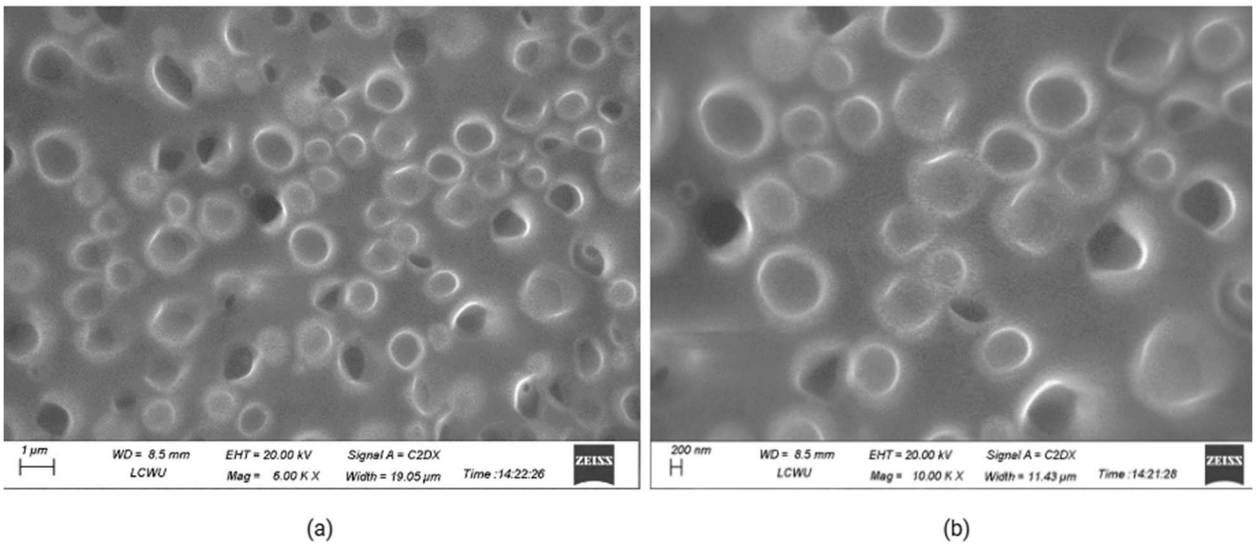

Fig. 8: Scanning Electron Microscopy (SEM) image of optimized mirtazapine-loaded transethosomes (F-16) showing spherical vesicles with smooth surfaces and uniform distribution. Scale bar at (a) 1 µm and (b) 200nm

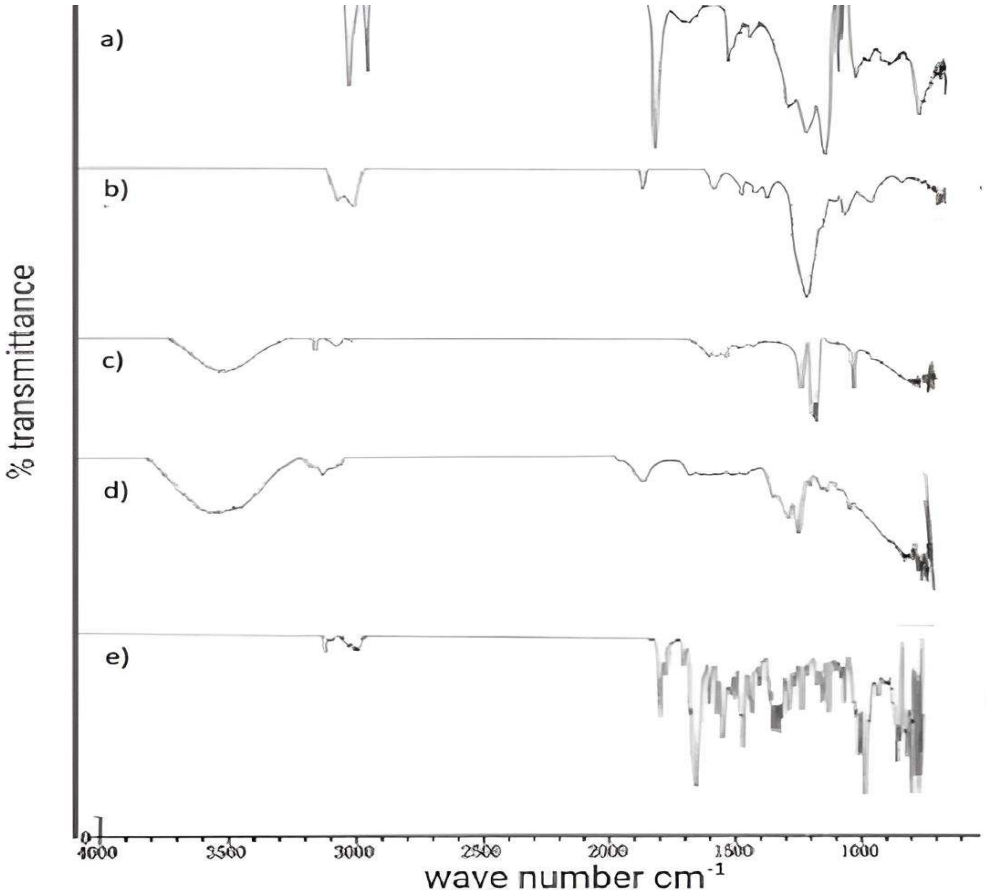

Fig. 9: FTIR spectrum of (a) soya lecithin, (b) Span 80, (c) ethanol, (d) mirtazapine, (e) mirtazapine loaded transethosomes

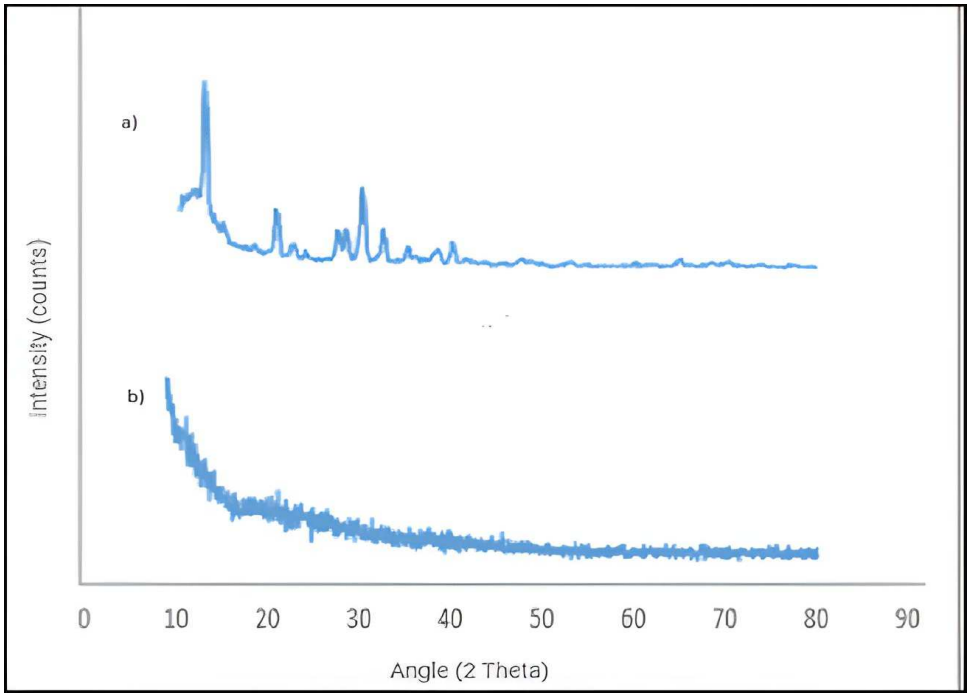

Fig. 10: XRD analysis of (a) pure drug and (b) Mirtazapine loaded transethosomes

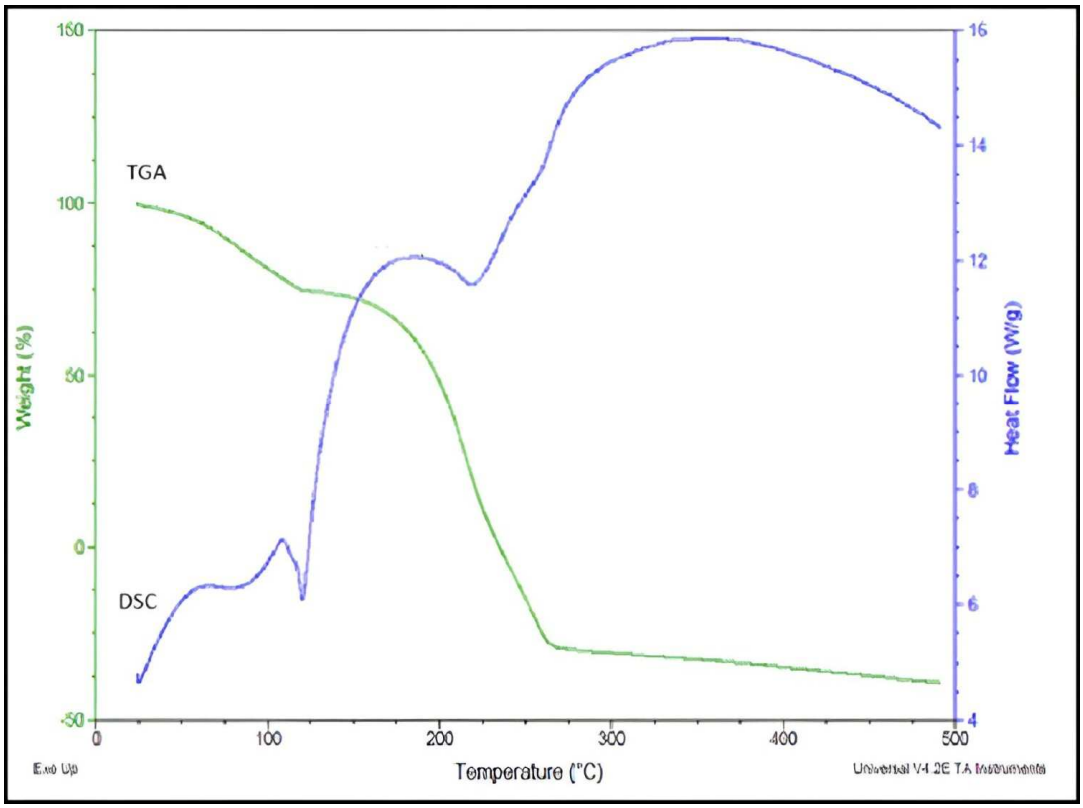

(a)

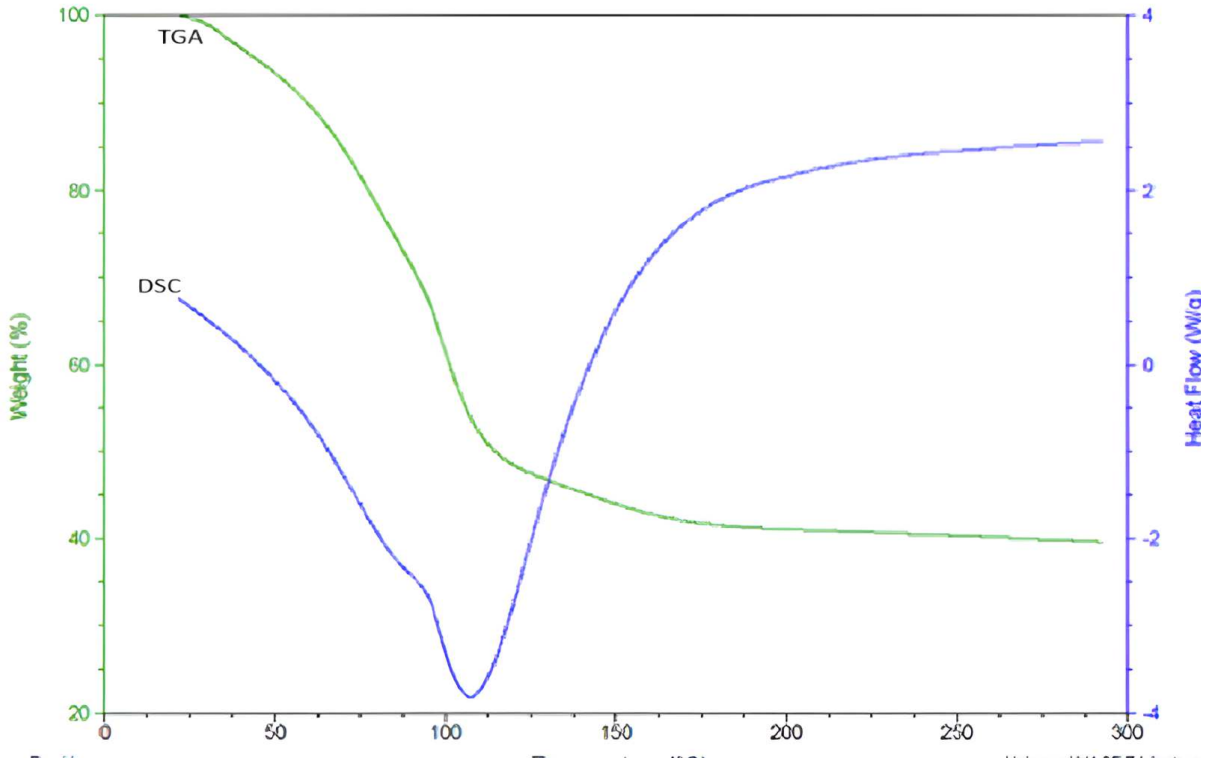

Fig. 11: DSC /TGA analysis of (a) the pure mirtazapine drug and (b) the mirtazapine loaded transethosomes

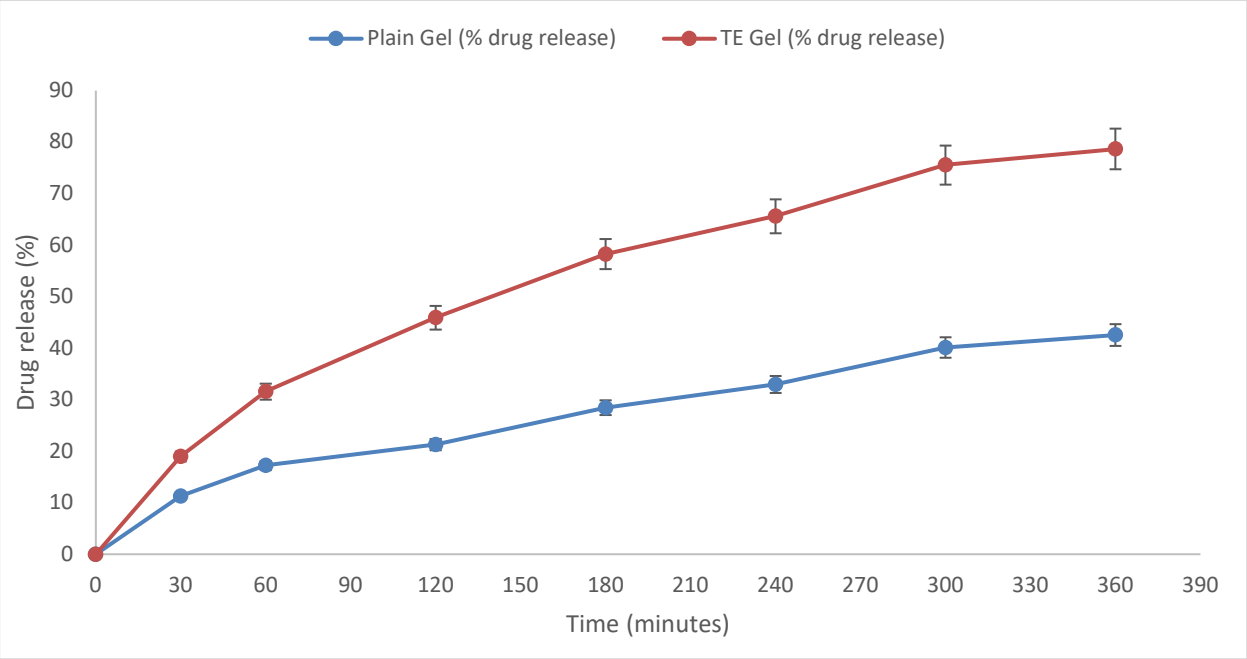

Fig. 12: Comparison of *in-vitro* drug release from transethosomal gel and plain gel

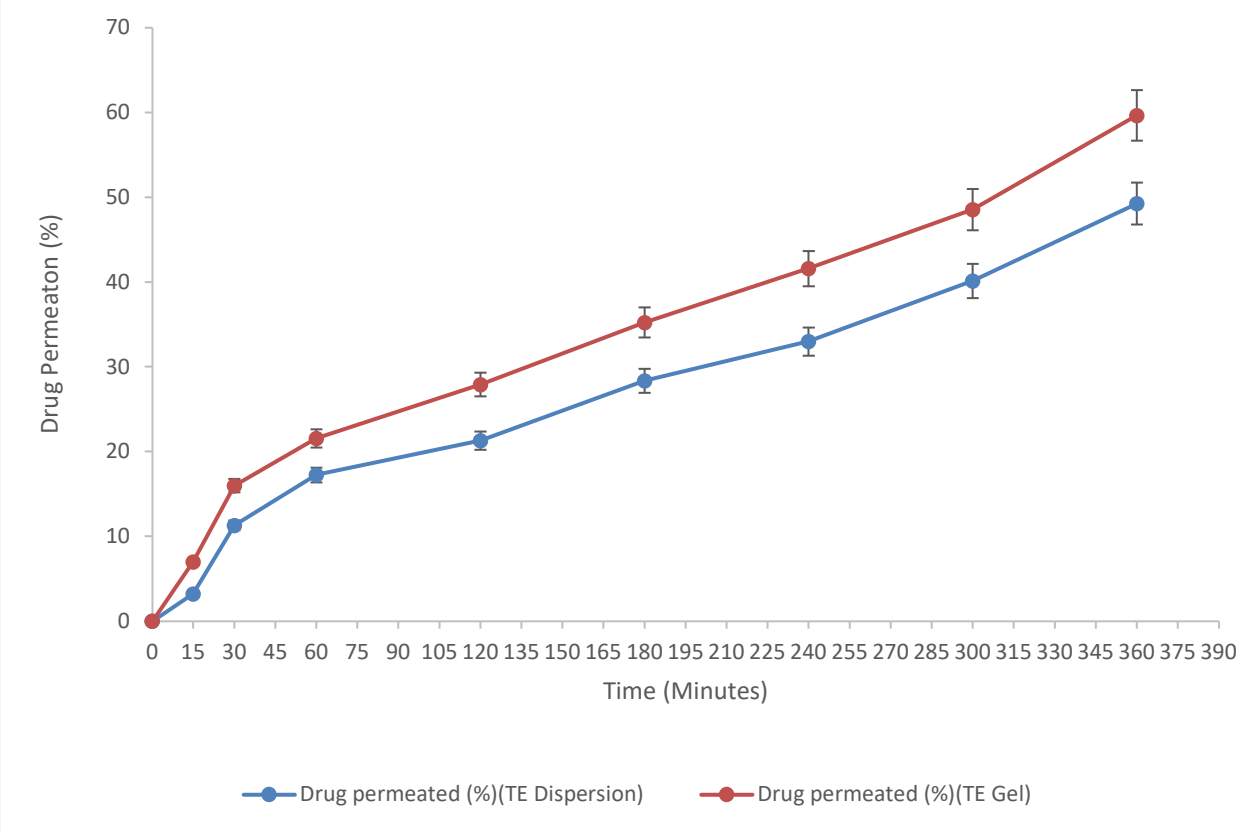

Fig. 13: Comparison of skin permeation through transethosomes dispersion and transethosomal gel

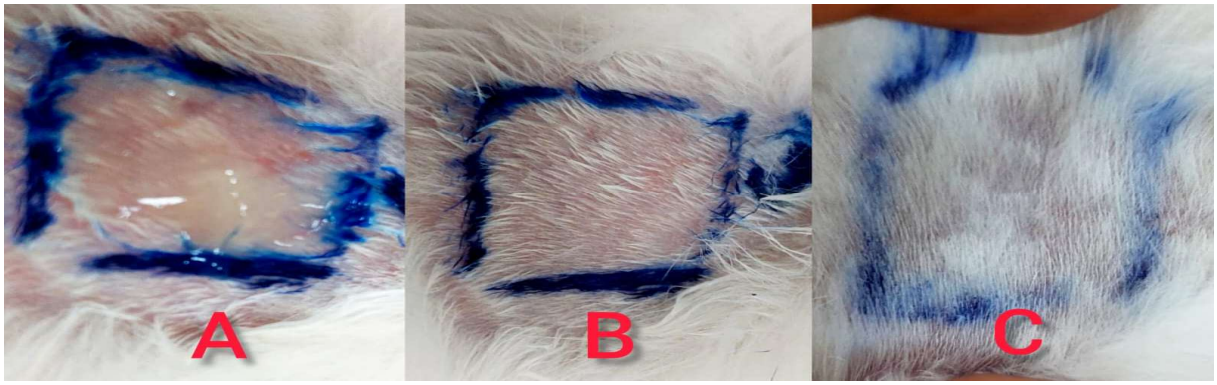

Fig. 14: Skin irritation study; (A) transethosomal gel is applied to the skin (B) rat skin after 24 hours of gel application (C) rat skin after three days of gel application

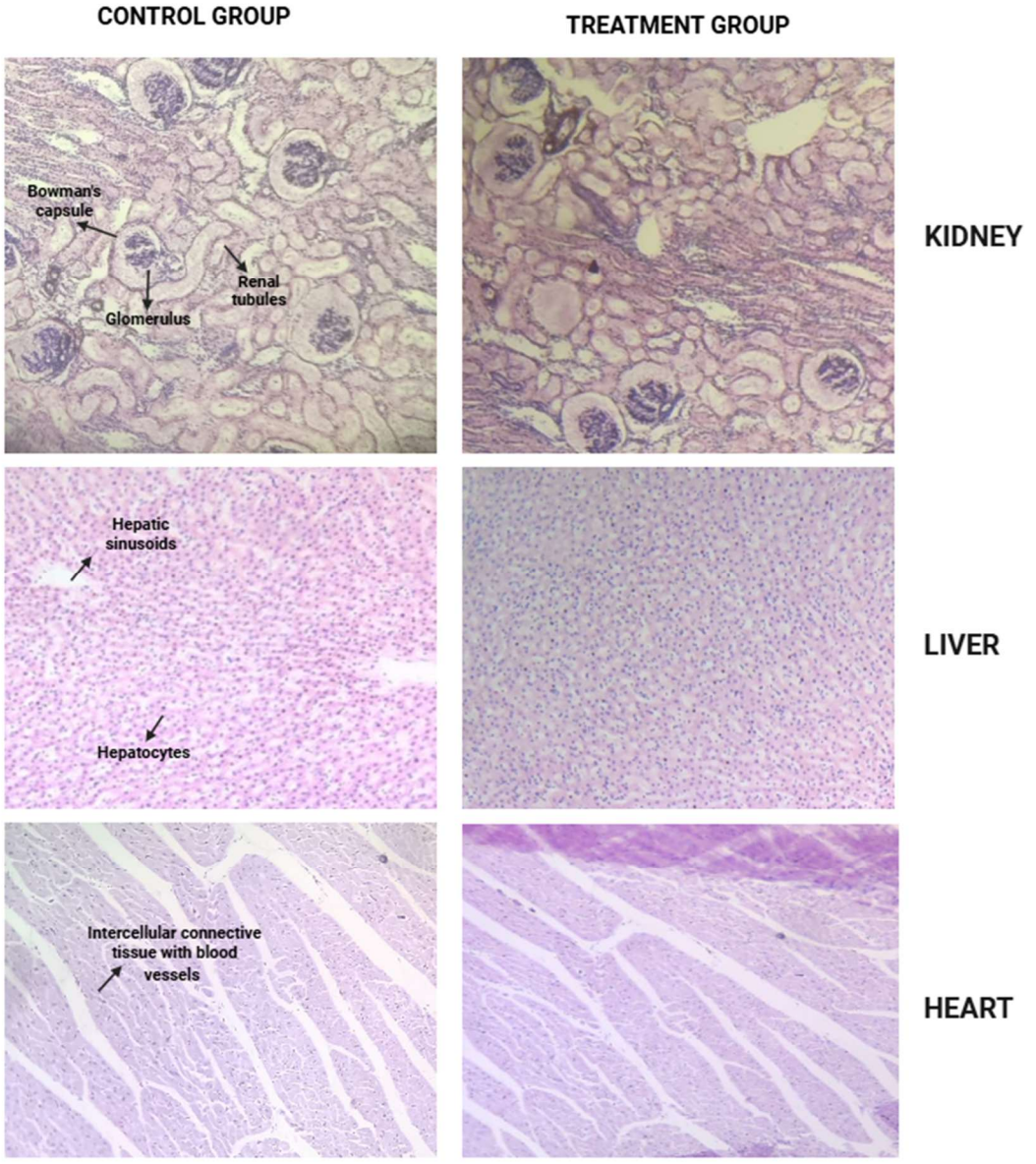

Fig. 15: Histopathological examination of rat skin following application of mirtazapine transethosomal gel. The epidermis and dermis appear intact with no signs of edema, inflammation, or structural disruption

Table 6: Summary of the result of regression analysis for responses Y_1 and Y_2

Quadratic model	R^2	Adjusted R^2	Predicted R^2	SD	%CV
Response (Y_1)	0.9959	0.9886	0.9351	0.69	0.96
Response (Y_2)	0.9986	0.9960	0.9770	0.68	1.03

Table 7: Summary of ANOVA

Source	Y_1			Y_2		
	F-value	p-value	Significance	F-value	p-value	Significance*
Model	136.42	< 0.0001*	Significant*	385.56	< 0.0001*	Significant*
A- Phospholipid	216.23	< 0.0001*		303.66	< 0.0001*	
B- Surfactant	324.84	< 0.0001*		12.73	0.0161*	
C- Ethanol	539.69	< 0.0001*		1850.87	< 0.0001*	
Residual						
Lack of Fit	2.40	0.7992		2.34	0.7792	

*Indicates statistical significance at P <0.05

Table 8: Drug release kinetics of transethosomal dispersion

	Zero order	First order	Higuchi	Korsmeyer-peppas		Hixson-Crowell
Mirtazapine loaded	R^2	R^2	R^2	R^2	n	R^2
transethosomal dispersion	0.7323	0.8048	0.8998	0.9038	0.55	0.7909

Table 9: Organoleptic Evaluation of prepared gel

Formulation	Color	Appearance	Homogeneity	Clarity	Texture	Stability
Mirtazapine TE Gel	Yellowish	Transparent	Homogeneous	Clear	Smooth, no lumps observed	No phase separation

Table 10: Stability study of Mirtazapine loaded TE gel (n=3, ±SD)

Temperature Condition	Time (Days)	Color	Clarity	Phase separation	Ph	Viscosity (cps)	Spreadability (g/s)	Drug content (%)
Room Temperature (25 ± 0.5 °C)	0	Yellowish	Clear	No	6.2±0.32	3540±0.45	27.60±0.69	91.28±1.63
	15	Yellowish	Clear	No	6.2±0.24	3540±0.24	27.56±0.83	91.22±1.24
	30	Yellowish	Clear	No	6.0±0.11	3531±0.38	27.50±0.97	91.19±1.28
	45	Yellowish	Clear	No	5.8±0.69	3524±0.13	27.46±1.02	91.14±1.86
	60	Yellowish	Clear	No	5.6±0.25	3506±0.81	27.35±0.65	91.10±2.04
Refrigerator Temperature (4 ± 0.5 °C)	0	Yellowish	Clear	No	6.2±0.58	3540±0.29	27.60±0.46	91.28±1.37
	15	Yellowish	Clear	No	6.2±0.37	3539±0.74	27.54±0.67	91.24±1.92
	30	Yellowish	Clear	No	5.6±0.14	3530±0.65	27.51±1.03	91.22±2.07
	45	Yellowish	Clear	No	5.4±0.29	3515±0.49	27.41±0.64	91.20±1.65
	60	Yellowish	Clear	No	5.0±0.47	3504±0.67	27.38±0.21	91.11±1.73

Response 1 (Y_1): effect of independent variables on the entrapment efficiency

By increasing the concentration of phospholipid, an increase in the entrapment efficiency is observed as shown in figs. 4 (a) and 4 (b). The reason could be the lipophilic character of mirtazapine because the drug which is lipophilic in nature would be deposited over the lipophilic phase. As shown in Table 2, the formulation F-3 which is composed of 2% phospholipid demonstrated an EE% of 75.6%, which is lower when compared to the formulation F-12 containing 4% phospholipid with an EE% of 77.9%. Same results were observed between formulation F-5 with 2% phospholipid (EE% of 61.6%) and formulation F-13 with 4% phospholipid (EE% of 67.8%). These results are consistent with the research conducted by Kumar et, al. in which Lipoid S100 is used as a lipid, and increased entrapment efficiency is seen by increasing the amount of lipid (Kumar and Utreja, 2020). In another study, by increasing the concentration of soya phosphatidylcholine 70, an increase in the entrapment efficiency is observed (Garg *et al.*, 2017).

The EE% is decreased by increasing the quantity of surfactant as shown in fig. 4(c). EE% of formulation F-3 (75.6%) which contains 10% surfactant is greater as compared to the EE% of formulation F-10 (63.3%) which contains 30% surfactant. In addition, formulation F-8 containing 10% surfactant and formulation F-15 containing 30% surfactant showed the entrapment efficiency of 86.5 % and 71.6% respectively. Same results

were observed between formulations F-12 and F-2. A rise in the concentration of surfactants can lead to the development of pores in the bilayer vesicles, causing the entrapped drug to escape out. A high concentration of surfactant can trigger the formation of micelles (Dantas *et al.*, 2016) and thus, the decrease in EE% with an increase in surfactant can be due to the coexistence of micelle structure with vesicles in the formulation as micelles usually show low entrapment efficiency as compared to vesicles (Aodah *et al.*, 2023)

Ethanol had a negative effect on the EE% of the transethosomes as demonstrated by the fig. 4(c). Formulation F-14 with 20% ethanol had an entrapment efficiency of 70.8%, but for formulation F-5 with 50% ethanol, it was 61.6%. The EE% was shown to be 86.5% for formulation F-8 with 20% ethanol, and 69.3% for formulation F-4 with 50% ethanol as shown in table 2. This decrease in the entrapment efficiency can be due to the fluidization mechanism of the ethanol. Ethanol increases the fluidity of the vesicles due to which there are more chances of drug leakage (Nayak *et al.*, 2020). These outcomes are consistent with the findings of research conducted by Moolakkadath *et al*., in which the increased concentration of ethanol decreased the encapsulation of transethosomes (Moolakkadath *et al.*, 2018).

Response 2 (Y_2): effect of independent variables on the amount of drug permeated after six hours

An increase in cumulative amount of the drug permeation by the increase in the concentration of the lipid could be because phospholipid could increase vesicle partitioning. Formulation F-2 contains 4% phospholipid has a Q6h of 65% which is greater than the Q6h of formulation F-10 (56.2 %) which contains 2% phospholipid. Additionally, similar findings were shown across formulations F-11 and F-14 and between formulation F-13 and F-5 which contains 4% and 2% phospholipid respectively (Nayak *et al.*, 2020).

An increase in the amount of drug permeated at Q6h is observed when the concentration of surfactants increases from 10% to 20% as shown in fig. 6. But by further increasing the concentration of surfactant from 20% to 30% decreases the Q6h. First, the increased surfactant concentration might have changed the packing characteristics of the bilayer, leading to the formation of a more disorganized and leakier vesicle membrane. Because of this, the vesicles are able to pass through skin pores more easily which would have increased drug permeability (Shen *et al.*, 2015). The decrease in the amount of drug permeated by further increasing the Span 80 concentration (from 20-30%) could be due to the micellar formation at high surfactant concentration.

Concentration of ethanol had a synergistic effect on the Q6h. Formulation F-15 which contains 20% ethanol shows less amount of drug permeated at Q6h (47.1 %) as compared to the formulation F-1 which shows the Q6h of 69.3%because of the higher concentration (50%) of ethanol. Likewise, Q6h was shown to be 63.9 %for formulation F-11 with 20% ethanol, and 86.7 %for formulation F-13 having 50% ethanol (Table 2). Ethanol is a penetration enhancer which decreased the transition temperature of lipid and gave the vesicles flexibility, which allowed the vesicles to penetrate through the skin (Tang *et al.*, 2007). Furthermore, ethanol increased the stratum corneum layer's fluidity and enhanced the ability of vesicles to pass through it by interacting with the lipids in the stratum corneum layer (El Maghraby, Williams and Barry, 2004).

Characterization of optimized transethosomes formulation (F-16)

Calibration curve

The standard calibration curve for mirtazapine (Fig. 6) exhibited strong linearity with a correlation coefficient (R^2) of 0.9987 and regression equation y = 0.0171x + 0.0627, indicating that the UV-VIS spectrophotometric method is linear and accurate across the tested concentration range (5–50 µg/ml) (Prajapati *et al.*, 2022).

Zeta potential, PDI and Particle size determination

The vesicle size of the prepared formulation was found to be 479.3 nm which confirms the nano-size of the prepared vesicles. Small vesicle size indicates the stable formulation. Optimized formulation showed the zeta potential of -34.1 mV as demonstrated in fig. 7. The formulation exhibited low polydispersity value of 0.400 that is generally acceptable and indicates the consistency of particle diameter within the formulation (Baboota *et al.*, 2007).

Scanning electron microscopy (SEM)

Particles are present in non-segregated form from each other and no agglomerates were observed. The prepared transethosomes appeared as almost spherical, homogenous, uni-lamellar nano-vesicles in the SEM pictures. The surface of the vesicle was smooth.

Drug excipients compatibility study

Soy lecithin's FTIR spectrum maximized at 1458.20 cm^{-1}, which is due to the (–CH2) bend. The carbonyl group (C=O) of phospholipids was seen in the spectrum at 1738.85 cm^{-1}. Peak at the 1054.11 cm^{-1} revealed phospholipid's (C–O-) stretch (Asghar *et al.*, 2023). Sorbian monooleate (Span 80), displayed a pattern of powerful distinctive absorption peak at 1173 cm^{-1} which is formed from the C–O–C stretching vibration (Fu *et al.*, 2015).The stretching vibration (O-H) peak trough in FTIR of ethanol is located at 3391 cm^{-1}. Ethanol was found to exhibit stretching vibrations (C-H) absorptions at wavenumbers ranging from 3010 cm^{-1} to 2850 cm^{-1}. Mirtazapine IR spectra showed N-H stretching at 3245 cm^{-1}. Mirtazapine's usual peaks were entirely suppressed

in mirtazapine transethosomes, showing that the drug was successfully entrapped within the vesicles.

X-ray diffraction (XRD) analysis

The diffractogram of pure mirtazapine in fig. 10 shows peaks at 9.54, 14.66, 20.24, 21.18, 22.38, 29.0, 30.52, 36.72 degrees and so on. The peaks confirmed the crystalline structure of the substance (Naureen *et al.*, 2022). However, the distinctive crystalline peaks of mirtazapine disappeared in the prepared formulation, producing a pattern of an amorphous material, confirming that the crystallinity of mirtazapine was significantly lowered, and thus confirms the conversion of crystalline form into the amorphous form in the final formulation.

Thermal stability analysis (DSC/TGA)

The TGA curve of pure mirtazapine (Fig. 11 a) showed an initial weight loss beginning at approximately 74 °C, with a significant mass loss occurring between 135–265 °C, which corresponds to the thermal degradation of the drug (Circioban *et al.*, 2024). The DSC thermogram displayed a single sharp endothermic peak around 254 °C, representing the melting point of crystalline mirtazapine. In the transethosomal formulation, this peak was significantly reduced in intensity and shifted to approximately 90–110°C (Fig. 11 b), indicating depression of the melting point due to interaction with excipients and a reduction in crystallinity (Kumbhar, Wavikar and Vavia, 2013). These results collectively confirm the partial amorphization and molecular dispersion of mirtazapine in the lipid matrix, which can enhance solubility and improve drug release performance.

Release kinetics

The results obtained through DD solver revealed that the R^2 value of mirtazapine loaded transethosomes was highest (0.9038) for the Korsmeyer-peppas model as shown in table 8. Also, the n value was higher than 0.5, which confirms that the drug release pattern follows the non-Fickian diffusion.

Characterization of the mirtazapine loaded transethosomal gel

Organoleptic Evaluation

The developed formulation had a yellowish color with no phase separation having a smooth and homogenous consistency and was free of any kind of grittiness and lumps.

pH, viscosity and spreadability

The pH of the transethosomal gel was measured using a digital pH meter. The pH of the gel was found to be 6.2 that was within the range of the pH of skin (i.e., 5.0 – 6.5) so it was considered non-irritant and safe for skin application. The rheological behavior of the prepared gel was determined because it influences the flow characteristics of the formulation during mixing, packaging into containers, storage, and application to the skin (Abdulbaqi *et al.*, 2018). The viscosity of the mirtazapine-loaded transethosomal gel was (3540 cp), which was considered acceptable and lies in the normal range. The spreadability of the transethosomal gel is important for uniform application of the formulation onto the skin. Spreadability of the formulated gel was found to be 27.60 g/s that was acceptable.

Drug content assessment

The results indicated that drug loss while preparing transethosomal gel was minimal and the drug is uniformly distributed throughout the formulation (Vasanth and Priya, 2024).

Drug release

Results clearly showed that the drug release from the transethosomal gel is greater than the plain mirtazapine gel as shown in fig. 12.

Ex-vivo permeation study

60% of the drug is permeated through the rabbit skin for six hours from the transethosomal gel. Drug permeation from transethosomal gel is greater which could be due to the colloidal characteristics of the gel such as the particle size, pH and viscosity. The ex-vivo permeation results demonstrated that approximately 60% of the loaded drug was released from the transethosomal gel within 6 hours. Given that the gel contains 0.45% w/w mirtazapine, and the therapeutic dose range for adults is 15–45 mg/day (Timmer *et al,.* 2000; Anttila and Leinonen, 2001), the observed drug flux from the optimized formulation indicates a potential for achieving therapeutic plasma concentrations. Furthermore, considering mirtazapine's long half-life (20–40 hours), sustained plasma levels could be maintained with once-daily transdermal application. While in-vivo pharmacokinetic studies are needed for confirmation, the ex-vivo release pattern strongly supports the transdermal route as a viable alternative to oral administration.

Stability studies

The results given in table 10 depicted that there were no major modifications in the color, viscosity, spreadability, homogeneity of the formulation following storage at both temperatures. Ph of the formulation slightly changed after 60 days at both temperatures. Furthermore, no major difference in the percentage drug content is observed between formulations held at 4 or 25°C when compared with the freshly prepared formulation. As a result, the data revealed that the mirtazapine loaded transethosomal gel was stable over the specified time period.

Skin irritation study

Rats showed no signs of erythema, skin rash, or edema (mean irritation index = 0) after the application of transethosomal gel as seen in fig. 14. As a result, the formulation was considered non-irritating and safe for application on the human skin. One of the limitations of

the current study is the short duration and small sample size (n=4 rats) used in the skin irritation assessment, which was conducted over a 3-day period. While no signs of erythema or edema were observed, these preliminary results should be interpreted cautiously. Longer-term studies with larger animal cohorts are recommended to confirm the dermal safety of the formulation prior to clinical translation

Toxicology and histopathology

Throughout the observation period, none of the rabbits displayed any physical changes or signs of sickness. There were no changes in the body weights of rabbits in both groups. There were no major changes in either the treatment or control groups throughout the two weeks as shown in the histopathological analysis as shown in the fig. 15. Vital organs such as the liver, heart and kidney were unaffected in both groups. The report of complete blood count (CBC) and levels of creatinine and urea were found to be within normal ranges. The level of Alanine aminotransferase (ALT) and Aspartate aminotransferase (AST) was also similar in control and treatment group. These measurements revealed no evidence of toxicity in the liver, kidney and blood in either group.

CONCLUSION

The present study successfully developed optimized mirtazapine-loaded transethosomal gel using Box–Behnken design, aiming to enhance transdermal delivery of the drug. The optimized formulation (F-16) demonstrated high entrapment efficiency (75.92%) and significant drug permeation after 6 hours (73.62%). Characterization studies confirmed nano-sized, stable vesicles with uniform morphology and effective drug encapsulation. The gel formulation exhibited suitable pH, viscosity, and spreadability, while ex-vivo skin permeation showed superior release from the gel compared to dispersion. Stability studies confirmed the formulation's robustness over 60 days. Importantly, toxicological and skin irritation analyses confirmed the formulation's safety profile. These findings suggest that the developed transethosomal gel is a promising transdermal delivery system for mirtazapine, potentially overcoming its poor oral bioavailability and offering improved patient compliance.

Acknowledgement

Not applicable

Authors' contributions

Faraz Ashraf: Lab work, Project resources, experimental trials and original draft; Hafiz Arfat Idrees: Primary investigator; Minahal Munir, Maaida Ajmal: Design analysis

Funding

There was no funding

Data availability statement

All data generated or analysed during this study are included in this published article [and its supplementary information files]. [Only use this if all data is in the manuscript or supplementary files.

Ethical approval

Ethical approval is provided by the "Institutional Research Ethics Committee" (REC) of the concerned department of the University of Lahore, Pakistan bearing ethical approval number IREC-2023-49 dated 26th October, 2023.

Conflict of interest

It has been verified that all the authors declare no conflict of interest.

REFERENCES

Abdallah MH, Elghamry HA, Khalifa NE, Khojali WM, Khafagy ES, Lila ASA, El-Horany HES and El-Housiny S (2022). Ginger extract-loaded sesame oil-based niosomal emulgel: Quality by design to ameliorate anti-inflammatory activity, *Gels*, **8**(11): 737.

Abdelnabi DM, Abdallah MH and Elghamry HA (2019). 'Buspirone hydrochloride loaded in situ nanovesicular gel as an anxiolytic nasal drug delivery system: *In vitro* and animal studies, *AAPS PharmSciTech*, **20**(3): 134.

Abdulbaqi IM, Darwis Y, Assi RA and Khan NAK (2018). 'Transethosomal gels as carriers for the transdermal delivery of colchicine: Statistical optimization, characterization, and ex vivo evaluation', *Drug des devel ther*, pp.795-813.

Acharya A, Ahmed MG and Rao BD (2016). Development and evaluation of ethosomal gel of lornoxicam for transdermal delivery: *in-vitro* and *in-vivo* evaluation, *MJPS.*, **2**(1): 3.

Akl MA, Eldeen MA and Kassem AM (2024). Beyond skin deep: Phospholipid-based nanovesicles as game-changers in transdermal drug delivery, *AAPS PharmSciTech*, **25**(6): 184.

Albash R, Abdelbary AA, Refai H and El-Nabarawi MA (2019). Use of transethosomes for enhancing the transdermal delivery of olmesartan medoxomil: in vitro, ex vivo, and *in vivo* evaluation, *Int. J. Nanomed.,***14**:1953-1968.

Anttila SA and Leinonen EV (2001). A review of the pharmacological and clinical profile of mirtazapine, *CNS drug reviews*, **7**(3): 249-264.

Aodah AH, Hashmi S, Akhtar N, Ullah Z, Zafar A, Zaki RM, Khan S, Ansari MJ, Jawaid T and Alam A (2023). Formulation development, optimization by box–behnken design, and *in vitro* and ex vivo characterization of hexatriacontane-loaded transethosomal gel for antimicrobial treatment for skin infections, *Gels*, **9**(4): 322.

Asad MI, Khan D, Rehman AU, Elaissari A and Ahmed N (2021). Development and *in vitro/in vivo* evaluation of pH-sensitive polymeric nanoparticles loaded hydrogel for the management of psoriasis', *Nanomaterials*, **11**(12): 3433.

Asghar Z, Jamshaid T, Sajid-ur-Rehman M, Jamshaid U and Gad HA (2023). Novel transethosomal gel containing miconazole nitrate; development, characterization, and enhanced antifungal activity, *Pharmaceutics*, **15**(11): 2537.

Baboota S, Shakeel F, Ahuja A, Ali J and Shafiq S (2007). Design, development and evaluation of novel nanoemulsion formulations for transdermal potential of celecoxib, *Acta Pharma.*, **57**(3): 315-332.

Bendale AR, Makwana JJ, Narkhede SP, Narkhede SB, Jadhav AG and Vidyasagar G (2011). Analytical method development and validation protocol for Lornoxicam in tablet dosage form, *JOCPR*, **3**: 258-263.

Bharate SS, Bharate SB and Bajaj AN (2010). Incompatibilities of pharmaceutical excipients with active pharmaceutical ingredients: A comprehensive review, *J. Excip. Food Chem.*, **1**(3): 3-26.

Circioban D, Ledeți A, Ridichie A, Vlase T, Ledeți I, Bradu IA, Pahomi A, Sbârcea L and Vlase G (2024). 'Compatibility study of mirtazapine with several excipients used in pharmaceutical dosage forms employing thermal and non-thermal methods, *J. Therm. Anal. Calorim.,* **150**(9):6747-6759.

Cong Z, Shi Y, Peng X, Wei B, Wang Y, Li J, Li J and Li J (2017). Design and optimization of thermosensitive nanoemulsion hydrogel for sustained-release of praziquantel, *Drug Dev. Ind. Pharm.,* **43**(4): 558-573.

Dantas MGB, Reis SAGB, Damasceno CMD, Rolim LA, Rolim-Neto PJ, Carvalho FO, Quintans-Junior LJ and Almeida JRGDS (2016). Development and evaluation of stability of a gel formulation containing the monoterpene borneol, *Sci. World J.,* **2016**(1): 7394685.

Demetzos C (2008) Differential scanning calorimetry (DSC): A tool to study the thermal behavior of lipid bilayers and liposomal stability, *J. Liposome Res.*, **18**(3): 159-173.

El-Menshawe SF, Ali AA, Halawa AA and Srag El-Din AS (2017). A novel transdermal nanoethosomal gel of betahistine dihydrochloride for weight gain control: *In-vitro* and *in-vivo* characterization, *Drug design, development and therapy*, **11**: 3377-3388.

El Maghraby G, Williams AC and Barry B (2004). Interactions of surfactants (edge activators) and skin penetration enhancers with liposomes, *Int. J. Pharm.*, **276**(1-2): 143-161.

Fang JY, Hwang TL, Huang YL and Fang CL (2006). Enhancement of the transdermal delivery of catechins by liposomes incorporating anionic surfactants and ethanol, *Int. J. Pharm.*, **310**(1-2): 131-138.

Franzé S, Donadoni G, Podestà A, Procacci P, Orioli M, Carini M, Minghetti P and Cilurzo F (2017). Tuning the
kin, *Mol Pharm.*, **14**(6): 1998-2009.

Fu X, Kong W, Zhang Y, Jiang L, Wang J and Lei J (2015). Novel solid–solid phase change materials with biodegradable trihydroxy surfactants for thermal energy storage, *Rsc Advances*, **5**(84): 68881-68889.

Gao S, Tian B, Han J, Zhang J, Shi Y, Lv Q and Li K (2019). Enhanced transdermal delivery of lornoxicam by nanostructured lipid carrier gels modified with polyarginine peptide for treatment of carrageenan-induced rat paw edema, *Inter. J. Nanomed.*, **14**: 6135-6150.

Garg V, Singh H, Bhatia A, Raza K, Singh SK, Singh B and Beg S (2017a). Systematic development of transethosomal gel system of piroxicam: formulation optimization, *in vitro* evaluation, and ex vivo assessment', *AAPS pharmscitech*, **18**(1): 58-71.

Gunasekara C, Law DW, Setunge S, Sanjayan JGJC and materials B (2015) Zeta potential, gel formation and compressive strength of low calcium fly ash geopolymers, **95**: 592-599.

Hamedi H, Moradi S, Tonelli AE and Hudson SM (2019). Preparation and characterization of chitosan–alginate polyelectrolyte complexes loaded with antibacterial thyme oil nanoemulsions, *Applied Sciences*, **9**(18): 3933.

Ho SC, Jacob SA and Tangiisuran B (2017). Barriers and facilitators of adherence to antidepressants among outpatients with major depressive disorder: A qualitative study, *PloS one*, **12**(6): e0179290.

Kadakia E, Shah L and Amiji MM (2017). Mathematical modeling and experimental validation of nanoemulsion-based drug transport across cellular barriers, *Pharm. res.*, **34**: 1416-1427.

Kaminsky BM, Bostwick JR and Guthrie SK (2015). Alternate routes of administration of antidepressant and antipsychotic medications, *Ann Pharmacother,* **49**(7): 808-817.

Kaur R, Sharma N, Tikoo K and Sinha V (2020). Development of mirtazapine loaded solid lipid nanoparticles for topical delivery: Optimization, characterization and cytotoxicity evaluation, *Int. J. Pharm.*, **586**: 119439.

Kumar L and Utreja P (2020). Formulation and characterization of transethosomes for enhanced transdermal delivery of propranolol hydrochloride, *Micro and nanosystems*, **12**(1): 38-47.

Kumbhar D, Wavikar P and Vavia P (2013). Niosomal gel of lornoxicam for topical delivery: *In vitro* assessment and pharmacodynamic activity, *AAPS pharmscitech*, **14**(3): 1072-1082.

Miastkowska M, Sikora E, Ogonowski J, Zielina M and Łudzik A (2016). The kinetic study of isotretinoin release from nanoemulsion, *Colloids and Surfaces A: Physicochemical and Engineering Aspects*, **510**: 63-68.

Moolakkadath T, Aqil M, Ahad A, Imam SS, Iqbal B, Sultana Y, Mujeeb M and Iqbal Z (2018). Development

of transethosomes formulation for dermal fisetin delivery: Box–Behnken design, optimization, *in vitro* skin penetration, vesicles–skin interaction and dermatokinetic studies, *Artif. Cells Nanomed. Biotechnol.*, **46**(sup2): 755-765.

Murata A, Kanbayashi T, Shimizu T and Miura M (2012). Risk factors for drug nonadherence in antidepressant-treated patients and implications of pharmacist adherence instructions for adherence improvement, *Patient Prefer. Adherence.,* **6**: 863-869.

Musallam AA, Mahdy M, Elnahas HM and Aldeeb RA (2022). Optimization of mirtazapine loaded into mesoporous silica nanostructures via Box-Behnken design: *In-vitro* characterization and *in-vivo* assessment, *Drug Delivery*, **29**(1): 1582-1594.

Naureen F, Shah Y, Shah SI, Abbas M, Rehman IU, Muhammad S, Goh KW, Khuda F, Khan A and Chan SY (2022). Formulation development of mirtazapine liquisolid compacts: Optimization using central composite design, *Molecules*, **27**(13): 4005.

Nayak D, Tawale RM, Aranjani JM and Tippavajhala VK (2020). Formulation, optimization and evaluation of novel ultra-deformable vesicular drug delivery system for an anti-fungal drug, *AAPS PharmSciTech*, **21**: 1-10.

Opatha SAT, Titapiwatanakun V and Chutoprapat R (2020). Transfersomes: A promising nanoencapsulation technique for transdermal drug delivery, *Pharmaceutics*, **12**(9): 855

Paiva-Santos AC, Silva AL, Guerra C, Peixoto D, Pereira-Silva M, Zeinali M, Mascarenhas-Melo F, Castro R and Veiga F (2021). Ethosomes as nanocarriers for the development of skin delivery formulations, *Pharm Res*, **38**(6): 947-970.

Pasaribu SP, Kaban J, Ginting M and Sinaga KR (2018). Synthesis and evaluation antibacterial activity of phosphate buffer solution (pH 7.4)-soluble acylated chitosan derivative. *AIP Conf. Proc.*, **2049**(1): 020025.

Pintea A, Vlad RA, Antonoaea P, Rédai EM, Todoran N, Barabás EC and Ciurba A (2022). Structural characterization and optimization of a miconazole oral gel, *Polymers*, **14**(22): 5011.

Pires PC, Mascarenhas-Melo F, Pedrosa K, Lopes D, Lopes J, Macário-Soares A, Peixoto D, Giram PS, Veiga F and Paiva-Santos AC (2023) Polymer-based biomaterials for pharmaceutical and biomedical applications: A focus on topical drug administration, *Eur. Polym. J.,* **187**: 111868.

Pires PC, Paiva-Santos AC and Veiga F (2023). Liposome-derived nanosystems for the treatment of behavioral and neurodegenerative diseases: The promise of niosomes, transfersomes and ethosomes for increased brain drug bioavailability, *Pharmaceuticals (Basel)*, **16**(10): 1424

Prajapati GM, Shinde AS, Pawar KA and Chavan KG (2022). Method development and validation for the estimation of mirtazapine by using UV spectrophotometer with different order of derivatives, *GSC Biol. Pharm. Sci.*, **19**(2): 196-204.

Puri A, Sivaraman A, Zhang W, Clark MR and Banga AK (2017). Expanding the domain of drug delivery for HIV prevention: Exploration of the transdermal route, *Crit Rev Ther Drug Carrier Syst.,* **34**(6): 551-587.

Qureshi MI, Jamil QA, Usman F, Wani TA, Farooq M, Shah HS, Ahmad H, Khalil R, Sajjad M and Zargar S (2023). Tioconazole-loaded transethosomal gel using box–behnken design for topical applications: *In vitro, in vivo*, and molecular docking approaches', *Gels*, **9**(9): 767.

Rai S, Pandey V and Rai G (2017). Transfersomes as versatile and flexible nano-vesicular carriers in skin cancer therapy: The state of the art, *Nano reviews & experiments*, **8**(1): 1325708.

Shah J, Nair AB, Jacob S, Patel RK, Shah H, Shehata TM and Morsy MA (2019) 'Nanoemulsion based vehicle for effective ocular delivery of moxifloxacin using experimental design and pharmacokinetic study in rabbits, *Pharmaceutics*, **11**(5): 230.

Shen Y, Ling X, Jiang W, Du S, Lu Y and Tu J (2015). 'Formulation and evaluation of cyclosporin A emulgel for ocular delivery, *Drug delivery*, **22**(7): 911-917.

Soliman WE, Shehata TM, Mohamed ME, Younis NS and Elsewedy HS (2021). Enhancement of curcumin anti-inflammatory effect via formulation into myrrh oil-based nanoemulgel. *Polymers*, **13**(4): 577.

Solmi M, Miola A, Croatto G, Pigato G, Favaro A, Fornaro M, Berk M, Smith L, Quevedo J and Maes M (2020). How can we improve antidepressant adherence in the management of depression? A targeted review and 10 clinical recommendations, *Braz. J. Psychiatry,* **43**: 189-202.

Song CK, Balakrishnan P, Shim CK, Chung SJ, Chong S and Kim DD (2012) A novel vesicular carrier, transethosome, for enhanced skin delivery of voriconazole: Characterization and *in vitro/in vivo* evaluation, *Colloids and surf. B: biointerfaces*, **92**: 299-304.

Sudhakar K, Fuloria S, Subramaniyan V, Sathasivam KV, Azad AK, Swain SS, Sekar M, Karupiah S, Porwal O and Sahoo A (2021). Ultraflexible liposome nanocargo as a dermal and transdermal drug delivery system, *Nanomaterials*, **11**(10): 2557.

Tang X, Zhu Y, Han L, Kim AL, Kopelovich L, Bickers DR and Athar M (2007). CP-31398 restores mutant p53 tumor suppressor function and inhibits UVB-induced skin carcinogenesis in mice, *J. Clin. Invest.,* **117**(12): 3753-3764.

Teleanu DM, Negut I, Grumezescu V, Grumezescu AM and Teleanu RI (2019). Nanomaterials for Drug Delivery to the Central Nervous System', *Nanomaterials (Basel)*, **9**(3): 371.

Timmer CJ, Sitsen JA and Delbressine LP (2000). Clinical pharmacokinetics of mirtazapine, *Clin. Pharmacokinet.,* **38**(6): 461-474.

Tiwari A, Bag P, Sarkar M, Chawla V and Chawla PA (2021). Formulation, validation and evaluation studies on metaxalone and diclofenac potassium topical gel, *Environ. Anal. Health Toxicol.,* **36**(1): e2021001.

Touitou E, Dayan N, Bergelson L, Godin B and Eliaz M (2000). Ethosomes—novel vesicular carriers for enhanced delivery: Characterization and skin penetration properties, *J. Control. Release,* **65**(3): 403-418.

Vasanth S and Priya S (2024). Bifonazole loaded transethosomal gel: Formulation and optimization by box behnken design, *Bull. Pharm. Sci. Assiut Univ.,* **47**(1): 65-81.

Vijayakumar R (2010). *Formulation and evaluation of diclofenac potassium ethosomes*. PhD diss., Madurai Medical College, Madurai.

Wu IY, Bala S, Skalko-Basnet N and Di Cagno MP (2019). Interpreting non-linear drug diffusion data: Utilizing Korsmeyer-Peppas model to study drug release from liposomes, *Eur. J. Pharm. Sci.,* **138**: 105026.

Yadav K, Rani A, Tyagi P and Babu MR (2023). The application of nanotechnology and nanomaterials in depression: An updated review, *Precision Nanomed*, **6**(2): 1023-1047.

Yıldız S, Aytekin E, Yavuz B, Bozdağ Pehlivan S and Unlu N (2016). Formulation studies for mirtazapine orally disintegrating tablets, *Drug Dev. Ind. Pharm.,* **42**(6): 1008-1017.